rijksuniversiteit groningen

Mechanical behavior of Cu-Ni core-shell nanowires

Bachelor Integration Project - Thesis

Frank Braaksma

University of Groningen
Faculty of Natural Sciences

June 2019

Supervisors:
Prof. A. Vakis
Prof. A.A. Geertsema
S. Solhjoo, PhD

f.h.braaksma@student.rug.nl
Student number: 1765256

Acknowledgements

This thesis was made possible with the help and support of several people, who I would like to thank in this section.

First, I must thank my supervisors, Prof. Antonis Vakis and Prof. Albert Geertsema, for providing me with feedback; insights; and solutions in all meetings and presentations.

I would also like to show my sincere gratitude to my daily supervisor, Soheil Solhjoo, PhD, for the weekly meetings containing numerous explanations, support and attention. Soheil was very kind and patient and assisted me with knowledge gaps I had.

I would like to thank the Center for Information Technology of the University of Groningen for their support and for providing access to the Peregrine high-performance computing cluster. Special thanks go out to Bob, who has answered all my queue, hardware and bash related questions in- and outside of working hours.

My thanks go out to my friends and family, who have lent an ear to my thoughts and presentations.

Most important, the guidance and continued moral support of Sigrid Broeze were instrumental in the finishing stages of this thesis, to which I am eternally grateful.

Abstract

Metallic nanowires have the potential to be or enhance the basic building blocks of nanomaterials. They are a key subject of research in the field of nanomaterials and nanocomposites. The subject of this research concerns the mechanical behavior of several ratios of Copper Nickel core-shell nanowires, a cylindrical composition of two nanomaterials. The mechanical behavior is determined using Molecular Dynamics simulated tensile tests on the nanowires. The tested nanowires have a length of 46 [nm], the diameter ranges from 7 to 25 [nm]. All nanowires were tensile tested for three strain velocities. The equilibration, tensile strength and deformation behavior were studied. The results show that single element nanowires have a higher ultimate tensile strength than core-shell nanowires. Tensile properties of the single element crystal nanowires are several times higher than the copper and nickel bulk materials. These tensile properties show that single element nanowires can be used to reinforce other nano- or macrostructures. A future application of these nanowires is therefore to enhance the mechanical behavior of other (nano)materials. The importance of the suggested research stems from the lack of available knowledge for copper nickel core-shell nanowires specifically and their comparison to pure element nanowires.

Layman's Summary

Metalen draden op nanoschaal is het onderwerp van deze scriptie. Dit type draden is de afgelopen 20 jaar een populair onderwerp van wetenschappelijk onderzoek. Deze populariteit komt door de unieke magnetische, elektrische en sterkte-eigenschappen. Voor dit onderzoek zijn computersimulaties gemaakt van draden met een kern van koper en een schil van nikkel. De draden in de simulatie zijn 46 nanometer lang en hebben een diameter van 7 tot 25 nanometer. Er zijn verschillende verhoudingen tussen de kern en de schil getest om uit te vinden welke samenstelling de hoogste treksterkte heeft. Uit het onderzoek is gebleken dat een nanodraad van alleen nikkel de hoogste treksterkte heeft. Van de draden met zowel koper als nikkel is van de geteste verhoudingen 15:10 het sterkst. De kristalstructuur binnenin de draden is onderzocht, hier is een verklaring gevonden voor deze resultaten. De draden veranderen intern van structuur, waardoor ze lokaal zwakker worden. Hierdoor breken ze sneller en hebben ze minder treksterkte. De draden van alleen nikkel zijn het best om andere nanomaterialen uit op te bouwen, ze kunnen ook gebruikt worden om bestaande materialen te verstevigen.

Table of Contents

List of Abbreviations

Abbreviation	Meaning	Page
NW	Nanowire	8
Cu	Copper	8
Ni	Nickel	8
FCC	Face-Centered Cubic	8
MD	Molecular Dynamics	8
FEA	Finite Element Analysis	9
FEM	Finite Element Method	9
Ag	Silver	10
LAMMPS	Large-scale Atomic/Molecular Massively Parallel Simulator	11
CPU	Central Processing Unit	11
GPU	Graphics Processing Unit	11
HPC	University of Groningen High-Performance computing Cluster	11
EAM	Embedded-Atom Model	12
OVITO	Open Visualization Tool	13
UTS	Ultimate Tensile Strength	20
HCP	Hexagonal Close-Packed	24
BCC	Body-Centered Cubic	24

1 Introduction

Metallic nanowires are miniscule structures, on a scale of 10^{-9} [m]. Nanowires (NWs) typically have a cylindrical form and are 1000 times longer than their diameter (Lefèvre, 2012). MIT associate professor of material science and engineering Silvija Gradečak categorizes NWs as "quasi-one-dimensional materials", because "two of their dimensions are on the nanometer scale" (Chandler, 2013). This quasi one-dimensionality provides NWs with (semi-)conductive, magnetic and mechanical properties different than their bulk counterparts (Guo, 2016; Wang, 2017). Because of this, the study of nanowire mechanics has gained significant scientific interest over the last two decades (Wang, Shan & Huang, 2017, Fig. 1). The size of the NWs ensures they have a wide range of applications, as they can serve as a connection between nanomaterials or nanostructures and materials on a macro-scale (Chandler, 2013). NWs are used to build nanostructures or enhance existing mechanical properties when applied to different materials and products. Existing applications are, for example, flexible OLED displays; Perovskite solar cells (Kim et al., 2018); and coating of titanium implants for medical use (Kim, Ng, Kunitake, Conklin & Yang, 2007). NWs created out of one element are thoroughly researched and documented (Sutrakar, 2008; Nayebi, 2010; Wang, 2017). However, there is a lack of knowledge on the mechanical behavior of core-shell nanowires and their comparison to pure element NWs. Core-shell NWs are composed of two different metals, which are combined to form one single NW. The inner core is composed of one metal, while the outer shell is another metal (Sarkar & Das, 2018). This research focuses on metallic core-shell nanowires, specifically Copper (Cu) and Nickel (Ni). These two metals were combined to form core-shell NWs. The inner core consists of Cu and the shell is made of Ni. Cu and Ni both are cubic crystal systems, with a Face-Centered Cubic (FCC) Bravais lattice structure (Callister & Rethwisch, 2007). The similarity in unit cell provided a good fit. Mechanical properties, such as the ultimate tensile strength and fracture point, were measured using simulated tensile tests through Molecular Dynamics (MD) simulations.

This section continues to explain the problem context, after which the problem statement is described. The existing body of literature is reviewed in Section 1.2, after which the research question is described.

1.1 Problem Context

For this thesis, due to time constraints, the choice was made to focus solely on the mechanical properties of metallic core-shell nanowires and their single element counterparts. Several experimental studies have been performed on the mechanical properties of single element NWs (Sutrakar, 2008; Sofiah, 2018). Sofiah, Samykano, Kadirgama, Mohan and Lah remarked about these experimental studies:

> Characterizing the mechanical properties of individual nanowires is a challenge to many current testing and measuring techniques. This is because the size is rather small, prohibiting the applications of the well-established testing techniques. For example, tensile testing requires that the size of the sample be sufficiently large to be clamped rigidly by the sample holder without sliding. This is impossible for metallic NW using conventional means. (2018, p. 325)

For this research, experimental tests of NWs' mechanical properties were not a viable option due to time constraints and complexity. As stated in the introduction, the choice was made to use MD simulations for the testing of the NWs. During the literature study it became evident that computer simulations have added and partly replaced the experimental studies.

1.1.1 Molecular Dynamics

Molecular Dynamics simulations describe the physical movement of atoms in atomistic or molecular systems. The simulations use discrete time, e.g. timesteps of a pre-determined length, and numerically solve Newton's equations of motion for the system (Alder & Wainwright, 1959). The drawback of solving equations numerically is that any error will be iterated as well. The cumulative error of these iterations can become substantial if the total time of the simulation is long, or the length of the timestep too great. To illustrate: to achieve a stable result with minimal errors, a timestep of 0.01 picosecond, 10^{-12} [s], was used for this research. Such a value is typical for MD simulations in general (Streett, Tildesley & Saville, 1978). One might expect current techniques and innovations to have replaced this method, such as the Finite Element Analysis (FEA). FEA uses the Finite Element Method (FEM), it is widely used in engineering and design to analyze thermodynamic properties, fluidic systems, mechanical behavior and electromagnetic properties (Logan, 2011). As Wackerfuß and Niederhöfer (2019) explain, the time integration of the FEM, used for these macro-scale simulations, is currently under development for use on the atomic scale. Hence, FEM is not suitable at this moment for data generation and testing on a nanoscale. It is specifically mentioned that the current MD codes and methods are highly developed and optimized for this type of research (Wackerfuß & Niederhöfer, 2019).

1.2 Literature review

The current state of knowledge about NWs is reviewed in this section. The literature review is concluded with research questions. These research questions are based on the gaps in the current body of knowledge.

1.2.1 Background

Nanowires are a part of the research field called Nanotechnology. It is defined by the U.S. National Nanotechnology Initiative as "The research and development efforts at the atomic or molecular level to create structures and systems applicable in diverse aspects" (Balzani, 2005). Nanotechnology as a research field is gaining significant scientific interest over the last two decades (Wang et al., 2017). One moment of inspiration for this field of science is traced back to a now famous talk of Richard Feynman at Caltech, USA. In December 1959, his lecture titled: 'There's plenty of room at the bottom: an invitation to enter a new world of physics', envisioned a powerful way to directly manipulate atoms (Feynman, 2018). Eric Drexler popularized this concept in the 1980s with his book 'Engines of Creation: The Coming Era of Nanotechnology' (Ball, Patil & Soni, 2019).

1.2.2 Studies

Multiple studies are performed on single-element NWs using MD simulations (Wu, 2006; Setoodeh, 2008; Huang, 2010; Kang, 2015). Core-shell NWs have been studied for their magnetic properties (Guo et al., 2016); conductive properties (Stewart, 2014; Kim, 2018); and mechanical properties (Ji, 2007; Jing, 2010; Sun, 2015). Previous research on core-shell NWs studied the effect of varying core diameter, shell thickness and strain velocity on the tensile properties of these core-shell NWs (Sarkar & Das, 2018). Results show that in copper-silver (Cu-Ag) core-shell NWs a lattice mismatch was present due to the difference in lattice constants (a_o) for Cu and Ag, 3.597 [Å] and 4.079 [Å] respectively (Davey, 1925). This difference in a_o resulted in internal tensile stresses applied to the Cu atoms and compressive stresses applied to the Ag atoms (Sarkar & Das, 2018). The suggested shell material for this research, Ni, has a_o = 3.499 [Å] (Davey, 1925). It is closer to the a_o value of Cu, which should result in fewer stresses applied inside the core-shell NW. The problem for this research is stated as: there is a lack of knowledge on the mechanical behavior of core-shell nanowires and their comparison to pure element nanowires. A disadvantage of using Cu is its tendency to oxidize at low temperature. It oxidizes fast and further oxidation is not prevented by a self-protective oxide layer (Li, Mayer & Colgan, 1991). Guo et al. (2016) synthesized Cu-Ni nanowire composites in a pentagonal shape and tested for magnetic properties. They state in their research that Ni acts an oxidation barrier for Cu, reinforcing the choice for Ni as a shell material and protective layer for Cu.

The literature review is concluded with the following summary: there exists a knowledge gap on the mechanical properties of cylindrical Cu-Ni core-shell NWs. This knowledge gap includes a comparison to their single element counterparts. The goal of this thesis is therefore: to find the ratio of core and shell in Cu-Ni core-shell NWs for optimized mechanical properties in tensile tests and compare this to their single element counterparts.

The following research question is derived: Which ratio of core to shell in Cu-Ni metallic core-shell nanowires provides the highest tensile strength in tensile tests?

To answer the main research question, the following sub questions are provided:

Which set of materials is best suited to use in the core-shell nanowire?

Cu and Ni were initially chosen to be used as materials. This first sub question is used to determine if these materials are the optimal choice to perform the tensile and bending tests on.

How can tensile tests be simulated using MD simulations?

Preliminary results show that the creation of a core-shell nanowire can be done using MD Simulations (see Appendix A). This question is used to find out how to perform the proposed tensile tests.

2 Methods and Tools

This section describes the program used for the MD simulations. To perform the simulation interatomic potentials are needed. Their theory and use will be explained as well. After this, the setup is clarified for generation, minimization, and equilibration of the materials. The completion of these three processes ensures that the given material is in an equilibrated state, ready to undergo the tensile tests.

2.1 Data acquisition

2.1.1 LAMMPS

Both the generation of needed data, and execution of tests are performed using the Large-scale Atomic/Molecular Massively Parallel Simulator (LAMMPS). This open-source software package performs MD simulations (Plimpton, 1995). These MD simulations are performed using a velocity-Verlet style integration for Newton's equations of motion (Verlet, 1967; Swope, 1982; Plimpton, 1995). LAMMPS is developed with the ability to use MD simulations on several Computer Processing Units (CPUs) or Graphics Processing Units (GPUs) in parallel. The simulations for this research were run on the University of Groningen High-Performance computing Cluster (HPC) for faster computation (Plimpton, 1995). The HPC is fitted with several GPU nodes, which were used for this thesis. The GPU package supported by LAMMPS decreased computation time for large-scale simulation (Brown, 2011; Brown, 2012). LAMMPS is widely used to perform MD simulations; it is well documented and able to use the NIST Interatomic Potentials Repository to describe materials.

2.1.2 Atomic Potentials

LAMMPS can use a variety of types of interatomic potentials to simulate atoms and their interaction with other atoms within the structure. A quantum mechanical calculation would provide the most accurate result, but these calculations are computationally expensive and therefore only viable to use with small scale simulations of 100 atoms or less (Onat & Durukanoglu, 2013). The Embedded-Atom Model (EAM) is developed to provide accurate results for use with metals and is computationally less expensive than quantum mechanical calculations (Daw, 1984; Foiles, 1985; Foiles, 1986; LeSar, 2013). The potential file used for the materials in this research is of this format. EAM potentials use a density functional theory. The total internal energy of the assembly of atoms U is calculated with the EAM method developed by Oh and Johnson (1988), using the following equations:

$$U = \sum_i E_i \tag{2.1}$$

$$E_i = F_i(\rho_i) + \frac{1}{2}\sum_{i=1}^{N}\sum_{j=1}^{N}\phi_{ij}(r_{ij}) \tag{2.2}$$

$$\rho_i = \sum_{j\neq i} f_{ij}(r_{ij}) \tag{2.3}$$

Where E_i is the internal energy associated with atom i, ρ_i is the total electron density at atom i. $F_i(\rho_i)$ is the amount of energy necessary to embed the atom i into the electron density. Atom i and j are separated by distance r_{ij}, $\phi_{ij}(r_{ij})$ is the potential of the pair of atoms. Lastly, $f_{ij}(r_{ij})$ is the contribution to the electron density at atom i from atom j, which is r_{ij} removed from atom i (Oh, 1988; LeSar, 2013). Using this model, Onat and Durukanoglu (2013) have developed a highly optimized potential for Cu and Ni within the formalisms of the EAM. This potential was determined by comparing the simulations performed to *ab initio* experimental data (Onat & Durukanoglu, 2013). This potential file was used in LAMMPS to provide the material properties for the Cu and Ni atoms during the MD simulations. The EAM lattice constant (a_o) is measured in Ångstrom [Å], which equals 10^{-10} [m]. Onat and Durukanoglu (2013) found for Cu and Ni a_o values of 3.615 and 3.520 [Å] respectively, which are provided in Table 1.

Table 1 – Lattice constant (a_o) for Cu and Ni in Angstrom from the EAM potential file created by Onat & Durukanoglu, 2013.

Material	a_o [Å]
Cu	3.615
Ni	3.520

The lattice constant describes the physical dimension of the unit cell in a crystal lattice. Cu and Ni both have an FCC structure, the sides of their cubic structure are equally

spaced and denoted by a_o (Callister & Rethwisch, 2007). The a_o value is used by LAMMPS to generate materials, together with the EAM potential file, see Appendix B and E for code examples.

2.2 Data preparation

Initially cubes of Cu and Ni were generated to determine minimization and temperature functions. The generation and equilibration of these cubes is found in Appendix B.

2.2.1 Generation of nanowires

The scope of the research is tensile tests of different core to shell, Cu and Ni respectively, ratios of nanowires using MD simulations. To aid in comparison of the data, the choice was made to base the dimensions of the NWs on the Cu-Ag dimensions of Sarkar and Das (2018). The length of the NWs for all simulations is therefore equal: 46 [nm]. In LAMMPS, cylinders consisting of Cu and Ni were generated, these cylinders are the NWs. For validation purposes the dimensions of NWs 2-6 were identical to the test performed by Sarkar and Das (2018) on copper-silver (Cu-Ag) nanowires. All NWs have a length of 46 [nm], the ratio of Cu to Ni ranges from a full Cu NW to a full Ni NW, see Table 2.

Table 2 - Core to shell ratios of the Cu-Ni core-shell nanowires to be generated and tested

Nanowire number	Cu core diameter [nm]	Ni shell thickness [nm]
1	25	0
2	23	2
3	21	4
4	19	6
5	17	8
6	15	10
7	5	2
8	10	2
9	15	2
10	20	2
11	0	12.5

All generated NWs are visualized using the Open Visualization Tool (OVITO), the top view of each NW is displayed in Figure 1 (Stukowski, 2009). A perspective view of each NW is included in Appendix C. The LAMMPS code used to generate the nanowires is provided in Appendix E.

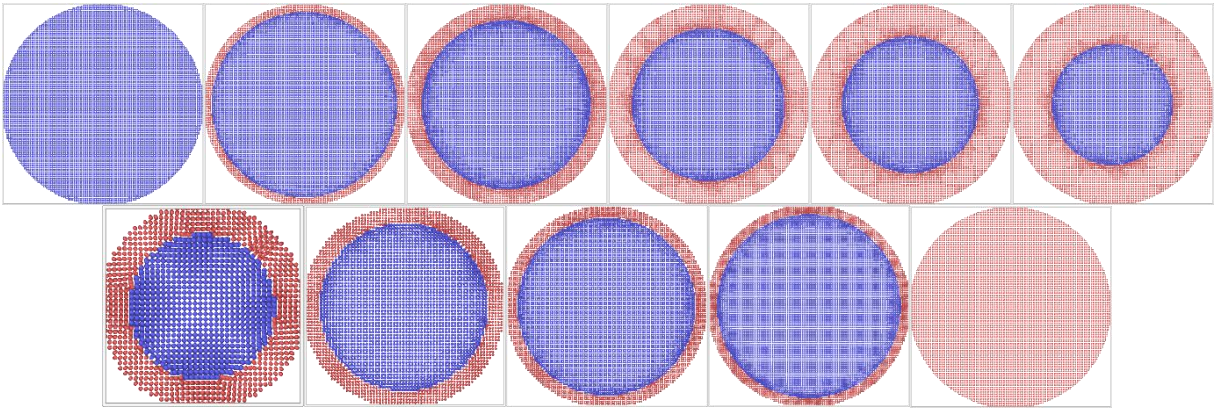

Figure 1 - Top view of all generated NWs. Top row, from left to right, NW 1-6. Bottom row, from left to right, NW 7-11. Core atoms are Cu (blue), shell atoms are Ni (red).

2.2.2 Equilibration

After generation of the NWs, all atoms are equally spaced and stationary. The aim of the research is to perform the simulated tensile tests at 300 [K]. First, the potential energy in the NW needs to be minimized. This minimization step is the first equilibration of the atoms. When an equilibrium is reached, temperature is added to the system. The system is then simulated until the temperature reaches an equilibrium: the total NW is equilibrated. Both processes are explained in more detail in the next subsections.

2.2.3 Minimization

After generation of the NWs, the first equilibration is minimizing the total potential energy in the system. In this process, LAMMPS iterates a function of the total amount of atoms N. The function used to perform this minimization is the Polak-Ribiere function of the conjugate gradient algorithm (Polak, 1969; Sandia, 2019). These iterations minimize the total potential energy of the system to obtain the lowest possible potential energy state. These iterations are continued until one of the stopping criteria is met.

The stopping criteria for the minimization in LAMMPS are 5 in total:

1. The change in total energy level between iterations is less than a specified value, the value used for the simulations is 1E-5 [-];
2. The length of the Force vector for the entire system is less than a specified value, the value used for the simulations is 1E-5 [eV/Å];
3. All atoms are stationary;
4. The minimization iterations have reached the allowed maximum, the set maximum for this research is 1000 iterations;
5. The number of force calculations have reached the allowed maximum, the set maximum for this research is 1000 iterations.

2.2.4 Temperature

After the minimization, temperature was added to the system using a canonical ensemble, where the number of atoms (N), volume (V) and temperature (T) remain the same during the simulation. The energies accumulated during the simulation are exchanged with a Nosé-Hoover thermostat in LAMMPS (Nosé, 1984; Hoover, 1985). The temperature was set to 300 [K] and the NWs simulated until the temperature equilibrated to a constant value.

2.3 Tensile test

The equilibrated NWs underwent a simulated tensile test. For this, the bottom and top rows of the atoms in the generated nanowires are fixed into position. This will be referred to as the fixed group. The fixed groups both span the NW in the x and y directions. For FCC Cu and Ni these are crystallographic directions [100] and [010] respectively. These fixed groups have a length of 20 [Å] in the z-axis, or [001] crystallographic direction, see Figure 2.

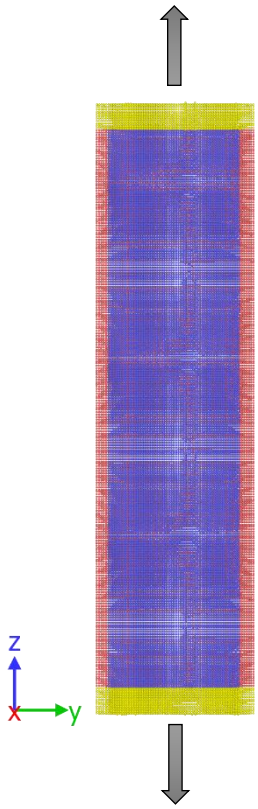

Figure 2 - Core-shell NW 8 with colorized fixed region (yellow). Core atoms are Cu (blue), shell atoms are Ni (red). Axial velocities applied during tensile test are indicated with arrows.

At timestep 0, t = 0 [ps], the NW is stationary with a velocity of 0 [Å/ps]. Subsequently, the fixed groups have a velocity applied in the z-axis, axial to the NW, see Figure 2. For each NW, three different velocities were simulated. Velocities of 0.2; 1.0 and 2.0 [Å/ps] were applied to the top fixed layer and -0.2; -1.0 and -2.0 [Å/ps] to the bottom fixed

layer respectively. This equates to three total strain velocities of 0.4; 2 and 4 [Å/ps]. Equations 2.4 and 2.5 show the calculation of strain and derivation of the strain rate.

$$\varepsilon(t) = \frac{L(t) - L(0)}{L(0)} \tag{2.4}$$

$$\dot{\varepsilon}(t) = \frac{d\varepsilon}{dt} = \frac{d}{dt}\left(\frac{L(t) - L(0)}{L(0)}\right) = \frac{1}{L_0}\frac{dL}{dt}(t) = \frac{v(t)}{L_0} \tag{2.5}$$

Where ε [-] is the dimensionless ratio of two lengths, describing the deformation with respect to time t [s]. $L(t)$ [m] is the length of the material at time t. $\dot{\varepsilon}$ [s^{-1}] is the derivative of ε; the rate at which strain develops over time. The strain rate is calculated by dividing velocity (v) by the length at t = 0 [s]. For the tensile test simulations, the velocity is known and constant. All NWs have an equal starting length of L_0 = 46 [nm]. For the total strain velocities in the axial direction of 0.4; 2 and 4 [Å/ps], the strain rates are 870, 4348 and 8696 [s^{-1}] respectively, see Table 3.

Table 3 - The three high strain rates used for tensile tests of NWs

Total strain velocity [Å/ps]	**Strain rate [s^{-1}]**
0.4	870
2	4348
4	8696

2.3.1 Simulation hardware

All NW simulations were performed on the University of Groningen Peregrine high-performance computing cluster. For generation, minimization and equilibration of the NWs simulation were performed on 2x Intel(R) Xeon(R) E5-2680 v3 @ 2.50GHz, accelerated with 2x Nvidia K40 GPUs. The tensile tests were performed on 1x Intel(R) Xeon(R) Gold 6150 @ 2.70GHz (virtualized), accelerated with 1x Nvidia V100 GPU.

2.4 Post-processing

This section describes the post-processing performed on the simulations to obtain the presented results.

2.4.1 LAMMPS output

The code used to generate the NWs outputs three files: a log file; a time-averaged text file and a dump file containing all atoms.

- Log file
  The log file is generated by LAMMPS during each simulation. It displays the code used to start the simulation, along with all intermediate steps taken. Every variable is calculated and displayed, along with any error messages. During this

research, the log file was mainly used for verification of successful simulations and troubleshooting failed simulations.

- Time-averaged text file
  The time-averaged text file was set to report averaged values over 10 timesteps, 100 [fs]. The variables averaged were the timestep; temperature; potential energy; strain; and forces acting on the fixed groups.
- Dump file
  The dump file, in its standard format, saves all information and used variables for each atom in the simulation for each timestep. For the generation and equilibration of the Cu and Ni cubes the standard setting was used. Generation and tensile tests of the NWs initially provided dump files of 100+ GB. For these tests, all atom data was stored in the dump file every 1000 timesteps.

Of these files, the dump file was used to study the behavior of the NWs visually using OVITO. The moment of fracture was determined and further study on movement; atom spacing; and crystal structure was performed.

2.4.2 Tensile forces

The time-averaged text file was used to track the temperature of the NW during the tensile test, along with the tensile forces generated within the NWs. LAMMPS calculated the tensile forces in electronVolt [eV] per Angstrom [Å] for each time step. The conversion to one MPa value for each nanowire was performed using the following dimensional analysis:

$$1\,\frac{eV}{\text{Å}} = \frac{1.6022 \cdot 10^{-19} J}{10^{-10} m} = 1.6022 \cdot 10^{-9} N \tag{2.6}$$

This provides two force values, F_T for forces acting upon the top fixed group and F_B acting on the bottom fixed group. These were averaged to find F_{avg} using the equation:

$$F_{avg} = \frac{F_T + F_B}{2} \tag{2.7}$$

The engineering stress was calculated using the following equation:

$$\sigma = \frac{F_{avg}}{A_0} \tag{2.8}$$

Where, for each time step, σ [Pa] is the resulting engineering stress, F_{avg} [N] the average force acting on the top and bottom fixed group and A_o [m²] the area of the NW.

2.4.3 Stress-strain

Using eq. 2.4 – 2.8, the stress and strain values were calculated. A moving average with a span of 0.005 was used in MATLAB to smooth the obtained results.

3 Results

3.1 Generation of Nanowires

Eleven NWs were generated using LAMMPS. All nanowires have a 46 [nm] length; the total diameter of NWs 1-6, and 11 is 25 [nm]. NWs 7-10 have a total diameter of 7, 12, 17 and 22 [nm] respectively. The total number of atoms generated by LAMMPS ranged from 155,880 atoms for NW 7 to 2,915,100 atoms for NW 6, see Table 4.

Table 4 - Variants of Cu-Ni NWs generated in LAMMPS, number of atoms created during the simulation and minimization iterations necessary to minimize total potential energy until a stopping criterium is met.

NW number	Number of generated atoms	Number of minimization iterations
1	1914788	3
2	1934912	38
3	1959590	40
4	1982450	48
5	1998200	51
6	2915100	49
7	155880	64
8	451655	49
9	901856	49
10	1501890	48
11	2073599	2

3.2 Minimization

The generated NWs were subsequently minimized using the LAMMPS minimization command, as described in section 2.2.3. All minimization functions stopped iterating due to meeting the first criterium. The amount of iterations necessary varied per NW, from 2 iterations for NW 11 to 64 iterations for NW 7, see Table 4.

3.3 Equilibration

After minimization the temperature was added to the entire system excluding the fixed layer. The fixed layer was set at 0 [K], while all other atoms were set at 300 [K]. The NWs were then simulated for 3000 timesteps, 30 [ps], to equilibrate. See Figure 3 for the temperature equilibration graph of NW 1, for graphs of NW 2-11 see Appendix C.

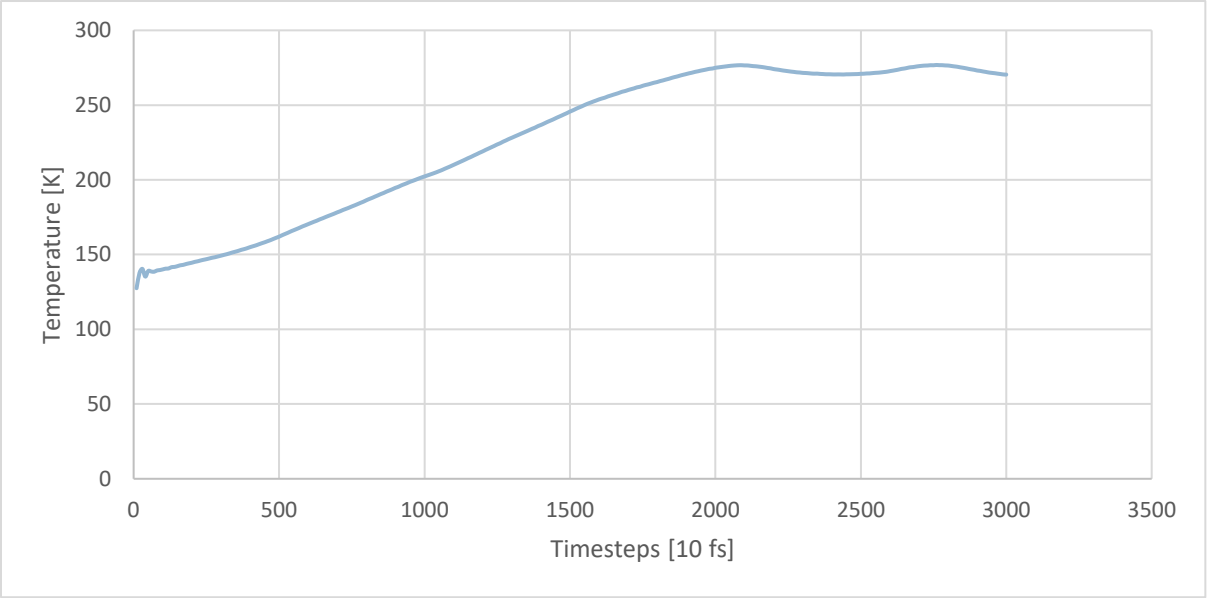

Figure 3 - Temperature [K] vs timestep [10 fs] graph, generated during equilibration of NW 1. Temperature equilibrates to approximately 270 [K].

3.4 Tensile Test

Tensile stress was applied to the generated NWs for three total strain velocities: 0,4; 2 and 4 [Å/ps], as described in section 2.3. The fracture point was visually determined using OVITO, see Figure 4.

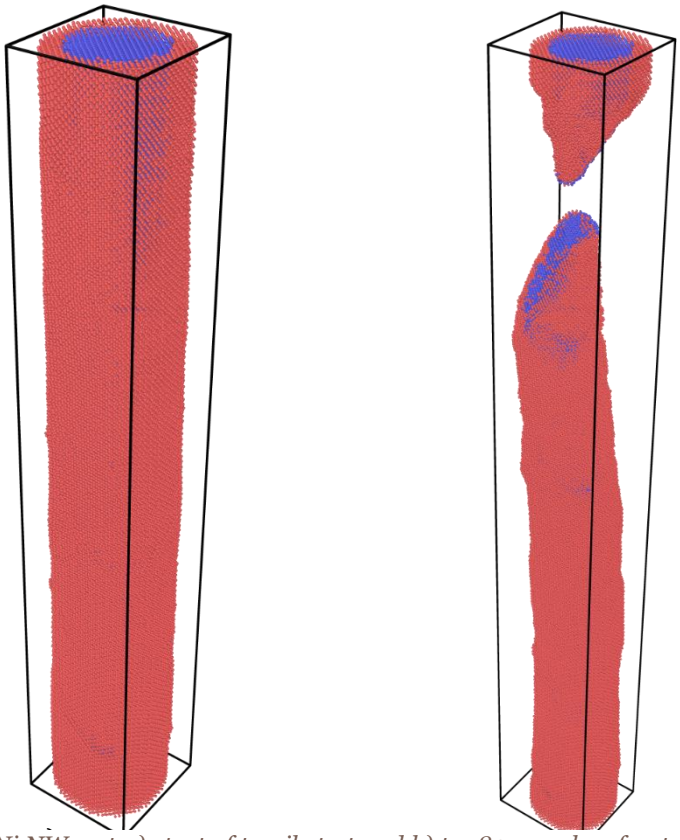

Figure 4 - Cu-Ni NW 7 at a) start of tensile test and b) t=580 ps, when fracture occurs. The core atoms are Cu (blue), the shell is Ni (red).

The highest force value was extracted from the time-averaged dump file, described in section 2.4.1. From the force value, the ultimate tensile strength (UTS) was calculated using equations 2.6 – 2.8 in section 2.4.2. The UTS occurs at a specific strain value, which were both reported for each NW. For total strain velocity of 0.4 [Å/ps], UTS values ranged from 3140 to 10335 [MPa], occurring at strain 0.050 and 0.088 [-] (NW 2 and 11 respectively). For total strain velocity of 2.0 [Å/ps], UTS values ranged from 4622 to 10745 [MPa], occurring at strain 0.081 and 0.090 [-] (NW 10 and 11 respectively). For total strain velocity of 4.0 [Å/ps], UTS values ranged from 5888 to 11570 [MPa], occurring at strain -3.64E-07 and 1.12E-01 [-] (for NW 1 and 11 respectively). All values are displayed in Table 5.

Table 5 – Ultimate Tensile Strength (UTS) [MPa], occurring at strain [-] for each NW. Values are reported for three total strain velocities: 0.4; 2.0; and 4.0 [A/ps].

		v_{tot} = 0.4 [Å/ps]		v_{tot} = 2.0 [Å/ps]		v_{tot} = 4.0 [Å/ps]	
NW	**Diameter [nm]**	**UTS [MPa]**	**Strain [-]**	**UTS [MPa]**	**Strain [-]**	**UTS [MPa]**	**Strain [-]**
1	25	5258	0.095	5909	0.102	5888	-3.64E-07
2	25	3140	0.050	4646	0.087	6308	1.74E-03
3	25	3311	0.049	4822	0.079	6417	2.52E-03
4	25	4060	0.055	5420	0.078	6579	1.56E-03
5	25	4483	0.055	6264	0.086	7041	3.56E-03
6	25	5023	0.061	6633	0.080	7626	2.70E-03
7	7	4831	0.092	5675	0.077	7776	4.69E-04
8	12	4205	0.051	6163	0.084	7610	1.74E-04
9	17	3525	0.050	4963	0.089	6842	1.74E-04
10	22	3077	0.047	4622	0.081	6832	1.52E-03
11	25	10335	0.088	10745	0.090	11570	1.12E-01

UTS and strain value for each NW are displayed in Figure 5.

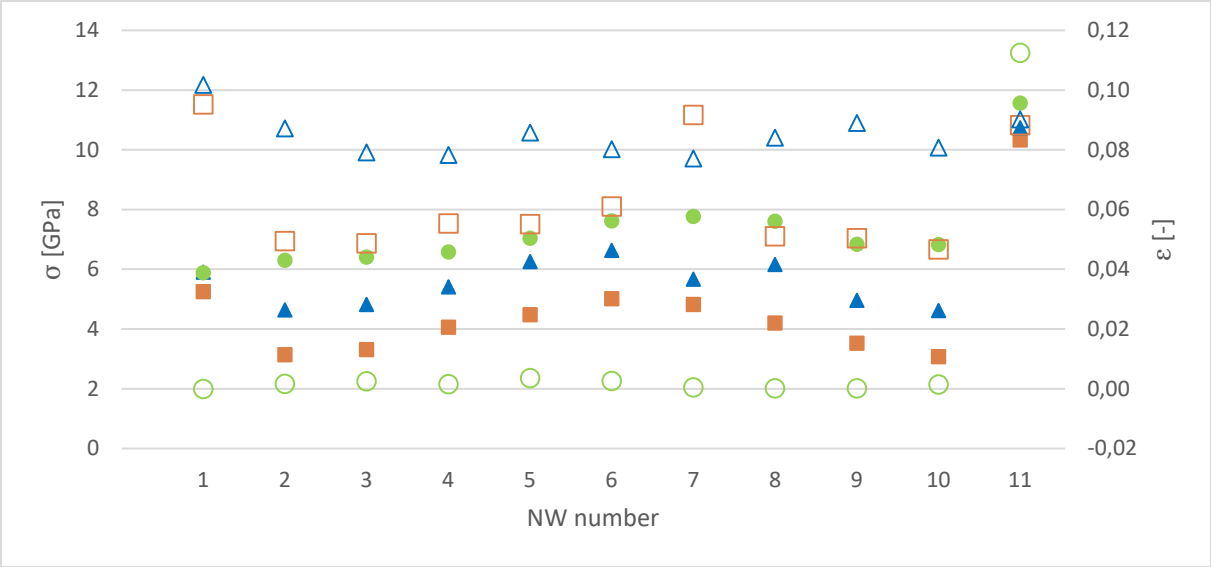

Figure 5 – Results of tensile tests performed on NWs: ultimate tensile strength in [GPa] (solid fill), occurring at strain value [-] (border only) for v_{tot}=0.4 (orange); 2.0 (blue) and 4.0 (green) [A/ps].

3.5 Temperature

The temperature of the NWs was monitored during the tensile tests, all NWs showed similar temperature graphs. Temperature graph of NW 6 is presented in Figure 6.

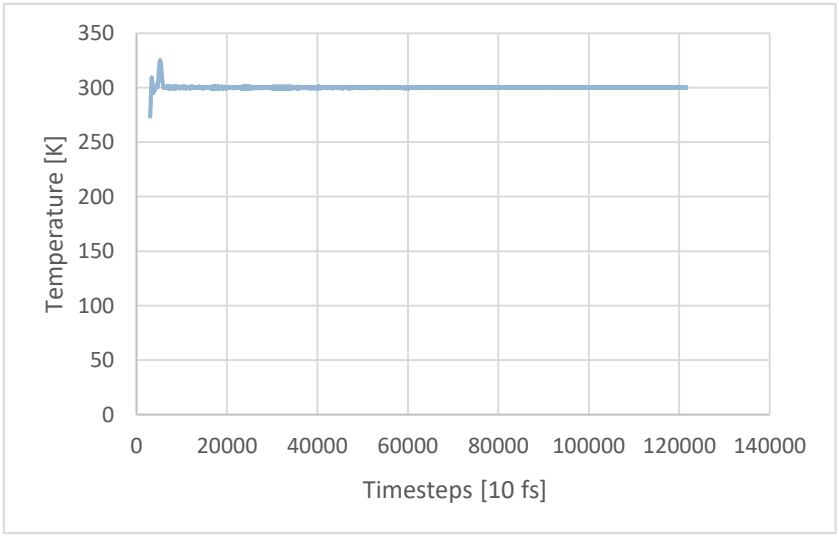

Figure 6 - Temperature [K] plotted against timesteps [10 fs], during tensile test simulation.

3.6 Stress-strain curves

The stress-strain values were calculated using the calculations described in section 2.4.3, after which they were smoothed and plotted. Stress-strain curves of NW 2 are plotted for all strain velocities, see Figure 7. Stress-strain curves for other NWs and strain velocities are displayed in Appendix F.

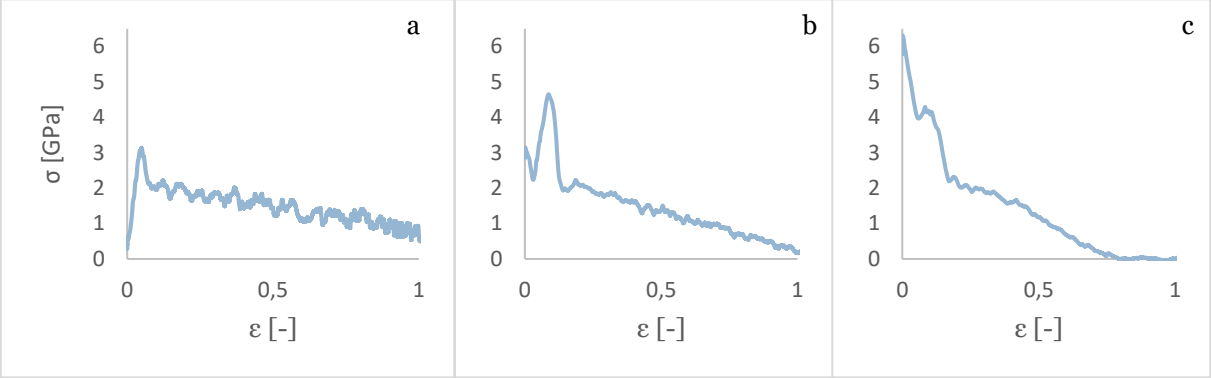

Figure 7 - Stress-strain curves of NW 2 during simulated tensile tests for strain velocity v_{tot}=0.4 (a); 2.0 (b) and 4.0 (c) [A/ps]. Stress values σ are given in GPa, strain ε in [-].

4 Discussion

Initially two simple cubic shapes from Cu and Ni were generated, see section 2.2. From Figures 12 and 13 in Appendix B it was concluded that the Cu and Ni cubes both can be equilibrated in a time span of 2000 timesteps using LAMMPS. These preliminary tests demonstrated that the used minimization and temperature functions were applicable to the Cu and Ni materials. It can be seen in both simulations at timesteps 0 and 1 that the temperatures fluctuate a large amount. The atoms are generated stationary at 0 [K], after which they are given a temperature of 300 [K], this causes the initial disturbance.

In section 3.4, the equilibration of NW 1 is visible. The temperature equilibrates to a temperature of ~270 [K]. This is lower than the temperature set to the NW, which is 300 [K]. This behavior appeared in all NWs, see Appendix C. The fixed groups in the NW have a velocity of 0 [Å/ps] and therefore a temperature of 0 [K]. The total length of all NWs is equal, 460 [Å]. The fixed groups have a total length of 20*2 = 40 [Å]. The ratio of free atoms to fixed atoms is 420 [Å]/460 [Å] = 0.913 [-]. If it is assumed that all atoms in the free region achieve 300 [K], the total temperature of the NW would be 300 [K] * 0.913 = 274 [K]. This is very close to the observed equilibrated temperature. The remaining difference in temperature could be explained as a result of the interactions between the fixed group and the free atoms. The atom interactions and energy define the total temperature in the NW. Due to the bottom and top fixed groups, there exist two stationary layers in the NW, see Figure 8.

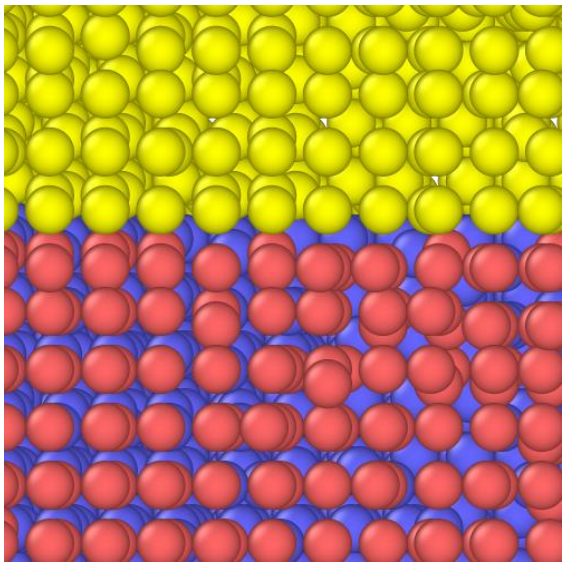

Figure 8 - Sliced view of boundary between top fixed atoms (yellow) and free Cu atoms (blue) and Ni atoms (red).

In Figure 8 the fixed atoms of the top group, colored yellow, are equally spaced due to the temperature of 0 [K]. The red and blue colored Cu and Ni atoms are disordered because of the 300 [K] temperature. The temperature gradient from the stationary fixed group to the free atoms explains the remaining temperature difference.

During the tensile tests, fracture propagation was monitored using OVITO. Sarkar and Das (2018), reported for the Cu-Ag NWs that failure behavior for strain velocities of 0.1 and 2 [Å/ps] was mainly ductile. For strain velocities higher than 2 [Å/ps] they denoted a ductile to brittle transformation (Sarkar & Das, 2018, Fig. 7). NW 8, with Cu core diameter of 10 [nm] and Ni shell thickness of 2 [nm], was studied visually for its deformation behavior, see Figure 9. For the strain velocity of 0.4 [Å/ps] (Figure 9a), ductile deformation behavior is visible. However, for the ultra-high strain velocity of 4.0 [Å/ps], the deformation is not as brittle as the Cu-Ag NW with similar dimensions, see Figure 9b. The difference in deformation behavior was explained using the Young's modulus (E) of Ag and Ni, these are 76 [GPa] and 207 [GPa] (Boyer & Gall, 1985). Ni is more ductile and therefore maintains ductile deformation behavior under higher strain velocities.

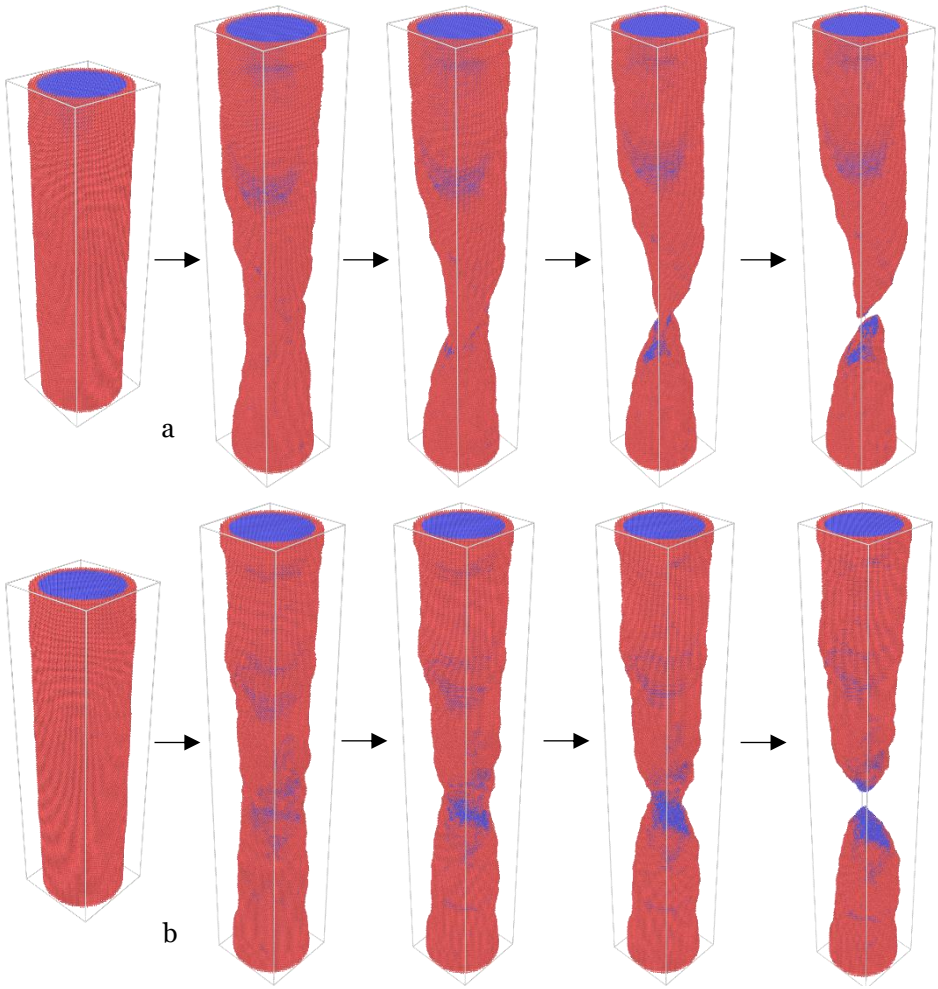

Figure 9 - Fracture propagation in NW 8 for strain velocity 0.4 [Å/ps] (a) and 4.0 [Å/ps] (b).

Ductile and brittle deformation behavior was further studied using polyhedral template matching in OVITO. All NWs exhibited changes in crystal structure over time during the tensile tests. NW 9 was examined in detail for all strain velocities. At t=0 [ps] of the tensile test, NW 9 still consists in large part of an FCC structure: 89,9%. The other reported structure types are Hexagonal Close-Packed (HCP): 2,0%, Simple cubic: 1,7%, Body-Centered Cubic (BCC): 0,2% and others: 6,2% (See Table 7, Figure 10a). NW 9 was visualized for all strain rates at strain ε = 0.6 [-] to study the influence of different strain rates on the crystal structure. For the total strain velocity v_{tot}= 0.4 [Å/ps], the following values were found. FCC: 85.8%, HCP: 4.4%, Simple cubic: 1.8%, BCC: 0.3% and others 6.2%. v_{tot} = 2 [Å /ps], FCC: 82.5%, HCP: 6.7%, Simple Cubic: 2.1%, BCC: 0.8% and others: 7.9%. Lastly, v_{tot} = 4 [Å /ps], FCC: 76.4%, HCP: 11.9%, Simple Cubic: 2.2%, BCC: 1.5% and others: 7.9%, see Table 6, Figure 10.

Table 6 - Reported crystal structures in NW 9 at t=0 and at strain value ε = 0.6 [-] for tensile test velocities 0.4, 2 and 4 [Å/ps].

Structure type	t=0 [%]	ε = 0.6, v = 0.4 [%]	ε = 0.6, v = 2 [%]	ε = 0.6, v = 4 [%]
FCC	89.9	85.8	82.5	76.4
HCP	2.0	4.4	6.7	11.9
Simple cubic	1.7	1.8	2.1	2.2
BCC	0.2	0.3	0.8	1.5
Others	6.2	7.7	7.9	7.9

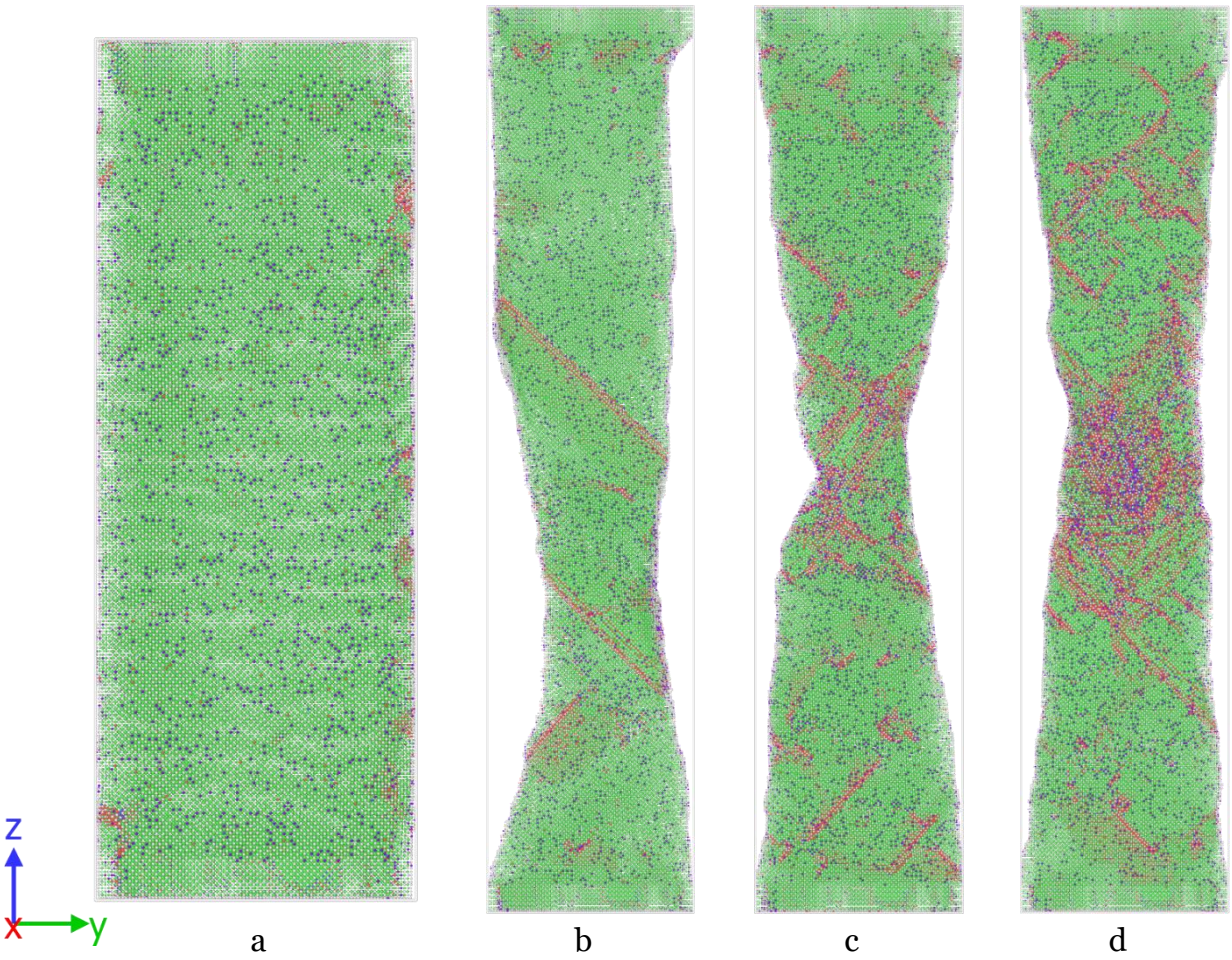

Figure 10 – Sliced view of NW 9 at t= 0 s (a) and ε = 0.6 [-] for v = 0.4; 1; and 2 [Å/ps] (b; c; and d respectively). Colors represent crystal structures: FCC (green), HCP (red), BCC (blue), Simple cubic (purple) and other (grey).

In Figure 10, the red HCP structure lines appear in 45-degree angles with respect to the loading direction. This can be explained by analyzing the slip systems of Cu and Ni. The tensile stress applied in the simulation is along the z-axis, or [001] direction of FCC Cu and Ni. The relation between the applied tensile stress σ and the shear stress τ_R on the NW is:

$$\tau_R = \sigma \cos(\lambda) \cos(\phi) \qquad (4.9)$$

Where λ is the angle between the force direction and the slip direction, and ϕ is the angle between the force direction and the normal to the slip plane (Callister & Rethwisch, 2007). When these planes slip, other crystal structures are formed. The HCP structure is most frequent around the necking region and is of specific interest. Slip in HCP is much more limited than in BCC and FCC crystal structures (Callister & Rethwisch, 2007). The NWs became more brittle in the region where HCP was prevalent. It was also visually confirmed with OVITO that fracture eventually occurs where the HCP structure is most frequent. From Table 6 and Figures 10b, c and d it is visible that for higher strain rates HPC was present in higher quantities. A 5 times increase in velocity, from 0.4 to 2.0 [Å/ps], provided a 52% higher formation of HPC, 4.4 and 6.7% respectively. Doubling the strain rate to 4.0 [Å/ps] resulted in an extra 77% increase in HPC structure. HPC has fewer slip directions than FCC or BCC, which resulted in a more brittle structure, localized in the central regions (Callister & Rethwisch, 2007).

The stress-strain curves of section 3.6 and Appendix F displayed several trends. For strain velocity 0.4 [Å/ps] all graphs start at 0 [GPa], show a rise to the UTS, after which the stress values started to fluctuate. For the high strain velocity 2.0 [Å/ps] similar behavior is visible, except all graphs start at 3.5-4.0 [GPa]. For the ultra-high strain velocity 4.0 [Å/ps] again similar behavior is visible after the peak of ε = 0.1 [-]. For this strain velocity, all graphs start at 6-7.5 [GPa], see Figures 18-24. In all NWs the stress gradually decreases and ultimately fails by necking.
The fluctuation in stress between the UTS and failure demonstrate the motion of the dislocations in the NW. The dislocations accumulated and shifting of structures transformed the NW from ductile to brittle. In the forming of these dislocations the force on the fixed groups fluctuated, this behavior is present in all NWs and in line with the findings of Sarkas and Das (2018).

From the UTS and strain values in Table 5, a comparison can be made to existing data for tensile strength of bulk Cu and Ni (Boyer and Gall, 1985), see Table 7.

Table 7 - Comparison between bulk Cu and Ni UTS values and UTS values obtained from tensile tests performed on NW 1 and 11.

Material	Bulk UTS [MPa]	NW UTS [MPa]
Cu	210	5258 – 5909
Ni	317	10335 – 11570

The UTS of the Cu and Ni NWs is found to be several times greater compared to their bulk equivalent. The NWs are highly ordered; the interface area of each atom is greater in comparison to the bulk material. A higher UTS is therefore expected, which is in line with findings from previous research (Sarkar & Das, 2018).

5 Conclusion

In this thesis, the mechanical behavior of Cu-Ni core-shell NWs at 300 [K] was estimated. The NWs had a length of 46 [nm], diameter varied from 7-25 [nm]. Using LAMMPS, tensile tests were simulated with Molecular Dynamics simulations for total strain velocities 0.4; 2 and 4.0 [Å/ps]. After generation, temperature was added to the NWs using a Nosé-Hoover thermostat. It was concluded that all generated NWs equilibrated to the desired temperature in 3000 timesteps, 30 [ps]. During the tensile test, temperature remained at 300 [K]. The main research question for this thesis was: which ratio of core to shell in Cu-Ni metallic core-shell nanowires provides the highest tensile strength in tensile tests? From the simulated tensile tests, the answer is: a NW consisting only of Ni has the highest ultimate tensile strength (UTS). In a core-shell configuration, a higher Ni/Cu ratio provides a higher UTS. The core-shell NW with a core diameter of 15 [nm] and 10 [nm] shell thickness shows the maximum UTS for strain velocities 0.4 and 2.0 [Å/ps]. For the ultra-high strain velocity of 4.0 [Å/ps], a core diameter of 5 [nm] and shell thickness of 2 [nm] showed the highest UTS. It is noted that with these high strain rates the composition of the crystal structure in the necking region changes from FCC to HPC. HPC has fewer slip directions than FCC; this creates a more brittle material, resulting in necking and failure. The UTS of single element NWs Cu and Ni were found to be greater than their bulk counterparts. The higher UTS was explained with highly ordered single crystal structures inside the NW, as opposed to coarse bulk materials. Hence, single element NWs of various dimensions are suitable for reinforcement of nano- or macrostructures.

Recommendations for further research are bending tests of the NWs to assess the flexural strengths and stresses. In this research the core was centered, asymmetrical core-shell NWs, with an off-center core could provide other useful directional properties. This could be simulated using only small adjustments to the simulation files from this thesis. Guo et al. (2016) have synthesized Cu-Ni pentagonal shaped NWs and tested magnetic properties. The pentagonal shape has a resemblance to the cylindrical NWs used in this research. The cylindrical NWs can be studied for their (semi)conductive and magnetic properties, for a direct comparison the shape of the MD simulated NWs could be made pentagonal.

6 References

Alder, B. J., & Wainwright, T. E. (1959). Studies in molecular dynamics. I. General method. *The Journal of Chemical Physics, 31*(2), 459-466.

Ball, A. S., Patil, S., & Soni, S. K. (2019). Introduction into nanotechnology and microbiology.

Balzani, V. (2005). Nanoscience and nanotechnology: a personal view of a chemist. *Small, 1*(3), 278-283.

Boyer, H. E., & Gall, T. L. (1985). Metals handbook; desk edition.

Brown, W. M., Kohlmeyer, A., Plimpton, S. J., & Tharrington, A. N. (2012). Implementing molecular dynamics on hybrid high performance computers–Particle–particle particle-mesh. *Computer Physics Communications, 183*(3), 449-459.

Brown, W. M., Wang, P., Plimpton, S. J., & Tharrington, A. N. (2011). Implementing molecular dynamics on hybrid high performance computers–short range forces. *Computer Physics Communications, 182*(4), 898-911.

Callister, W. D., & Rethwisch, D. G. (2007). *Materials science and engineering: an introduction* John Wiley & Sons New York.

Chandler, D. L. (2013). *Explained: Nanowires and nanotubes*. Retrieved 6/15, 2019, from http://news.mit.edu/2013/explained-nanowires-and-nanotubes-0411

Davey, W. P. (1925). Precision measurements of the lattice constants of twelve common metals. *Physical Review, 25*(6), 753.

Daw, M. S., & Baskes, M. I. (1984). Embedded-atom method: Derivation and application to impurities, surfaces, and other defects in metals. *Physical Review B, 29*(12), 6443.

Feynman, R. (2018). There's plenty of room at the bottom. *Feynman and computation* (pp. 63-76) CRC Press.

Foiles, S. (1985). Calculation of the surface segregation of Ni-Cu alloys with the use of the embedded-atom method. *Physical Review B, 32*(12), 7685.

Foiles, S., Baskes, M., & Daw, M. S. (1986). Embedded-atom-method functions for the fcc metals Cu, Ag, Au, Ni, Pd, Pt, and their alloys. *Physical Review B, 33*(12), 7983.

Guo, H., Jin, J., Chen, Y., Liu, X., Zeng, D., Wang, L., et al. (2016). Controllable synthesis of Cu–Ni core–shell nanoparticles and nanowires with tunable magnetic properties. *Chemical Communications, 52*(42), 6918-6921.

Hoover, W. G. (1985). Canonical dynamics: Equilibrium phase-space distributions. *Physical Review A, 31*(3), 1695.

Huang, D., & Qiao, P. (2010). Mechanical behavior and size sensitivity of nanocrystalline nickel wires using molecular dynamics simulation. *Journal of Aerospace Engineering, 24*(2), 147-153.

Ji, C., & Park, H. S. (2007). Characterizing the elasticity of hollow metal nanowires. *Nanotechnology, 18*(11), 115707.

Jing, Y., & Meng, Q. (2010). Molecular dynamics simulations of the mechanical properties of crystalline/amorphous silicon core/shell nanowires. *Physica B: Condensed Matter, 405*(10), 2413-2417.

Kang, M., Lee, H., Kang, T., & Kim, B. (2015). Synthesis, properties, and biological application of perfect crystal gold nanowires: a review. *Journal of Materials Science & Technology, 31*(6), 573-580.

Kim, K., Kwon, H., Ma, S., Lee, E., Yun, S., Jang, G., et al. (2018). All-Solution-Processed Thermally and Chemically Stable Copper–Nickel Core–Shell Nanowire-Based Composite Window Electrodes for Perovskite Solar Cells. *ACS Applied Materials & Interfaces, 10*(36), 30337-30347.

Kim, W., Ng, J. K., Kunitake, M. E., Conklin, B. R., & Yang, P. (2007). Interfacing silicon nanowires with mammalian cells. *Journal of the American Chemical Society, 129*(23), 7228-7229.

Lefèvre, V. (2012). *Nanowires: Properties, Synthesis, and Applications* Nova Science Publishers.

LeSar, R. (2013). *Introduction to computational materials science: fundamentals to applications* Cambridge University Press.

Li, J., Mayer, J., & Colgan, E. (1991). Oxidation and protection in copper and copper alloy thin films. *Journal of Applied Physics, 70*(5), 2820-2827.

Logan, D. L. (2011). *A first course in the finite element method* Cengage Learning.

Nayebi, P., Shamshirsaz, M., & Zaminpeyma, E. (2010). Molecular dynamics simulation of mechanical properties of gold nanowire. *2010 Symposium on Design Test Integration and Packaging of MEMS/MOEMS (DTIP),* pp. 3-5.

Nosé, S. (1984). A unified formulation of the constant temperature molecular dynamics methods. *The Journal of Chemical Physics, 81*(1), 511-519.

Oh, D., & Johnson, R. (1988). Simple embedded atom method model for fcc and hcp metals. *Journal of Materials Research, 3*(3), 471-478.

Onat, B., & Durukanoğlu, S. (2013). An optimized interatomic potential for Cu–Ni alloys with the embedded-atom method. *Journal of Physics: Condensed Matter, 26*(3), 035404.

Plimpton, S. (1995). Fast parallel algorithms for short-range molecular dynamics. *Journal of Computational Physics, 117*(1), 1-19.

Polak, E., & Ribiere, G. (1969). Note sur la convergence de méthodes de directions conjuguées. *ESAIM: Mathematical Modelling and Numerical Analysis-Modélisation Mathématique Et Analyse Numérique, 3*(R1), 35-43.

Sandia National Labs. (2019). *minimize command.* Retrieved Jun 15, 2019, from https://lammps.sandia.gov/doc/minimize.html

Sarkar, J., & Das, D. (2018). Study of the effect of varying core diameter, shell thickness and strain velocity on the tensile properties of single crystals of Cu–Ag core–shell nanowire using molecular dynamics simulations. *Journal of Nanoparticle Research, 20*(1), 9.

Setoodeh, A., Attariani, H., & Khosrownejad, M. (2008). Nickel nanowires under uniaxial loads: A molecular dynamics simulation study. *Computational Materials Science, 44*(2), 378-384.

Sofiah A. G. N., Samykano, M., Kadirgama, K., Mohan, R. V., & Lah, N. A. C. (2018). Metallic nanowires: Mechanical properties - Theory and experiment. *Applied Materials Today, 11*, 320-337.

Solhjoo, S., & Vakis, A. I. (2015). Definition and detection of contact in atomistic simulations. *Computational Materials Science, 109*, 172-182.

Stewart, I. E., Rathmell, A. R., Yan, L., Ye, S., Flowers, P. F., You, W., et al. (2014). Solution-processed copper–nickel nanowire anodes for organic solar cells. *Nanoscale, 6*(11), 5980-5988.

Streett, W., Tildesley, D., & Saville, G. (1978). Multiple time-step methods in molecular dynamics. *Molecular Physics, 35*(3), 639-648.

Stukowski, A. (2009). Visualization and analysis of atomistic simulation data with OVITO–the Open Visualization Tool. *Modelling and Simulation in Materials Science and Engineering, 18*(1), 015012.

Sun, J., Fang, L., Ma, A., Jiang, J., Han, Y., Chen, H., et al. (2015). The fracture behavior of twinned Cu nanowires: A molecular dynamics simulation. *Materials Science and Engineering: A, 634*, 86-90.

Sutrakar, V. K., & Mahapatra, D. R. (2008). Formation of stable ultra-thin pentagon Cu nanowires under high strain rate loading. *Journal of Physics: Condensed Matter, 20*(33), 335206.

Swope, W. C., Andersen, H. C., Berens, P. H., & Wilson, K. R. (1982). A computer simulation method for the calculation of equilibrium constants for the formation of physical clusters of molecules: Application to small water clusters. *The Journal of Chemical Physics, 76*(1), 637-649.

Verlet, L. (1967). Computer" experiments" on classical fluids. I. Thermodynamical properties of Lennard-Jones molecules. *Physical Review, 159*(1), 98.

Wackerfuß, J., & Niederhöfer, F. (2019). Using finite element codes as a numerical platform to run molecular dynamics simulations. *Computational Mechanics, 63*(2), 271-300.

Wang, S., Shan, Z., & Huang, H. (2017). The mechanical properties of nanowires. *Advanced Science, 4*(4), 1600332.

Wu, H. (2006). Molecular dynamics study of the mechanics of metal nanowires at finite temperature. *European Journal of Mechanics-A/Solids, 25*(2), 370-377.

Appendices

Appendix A

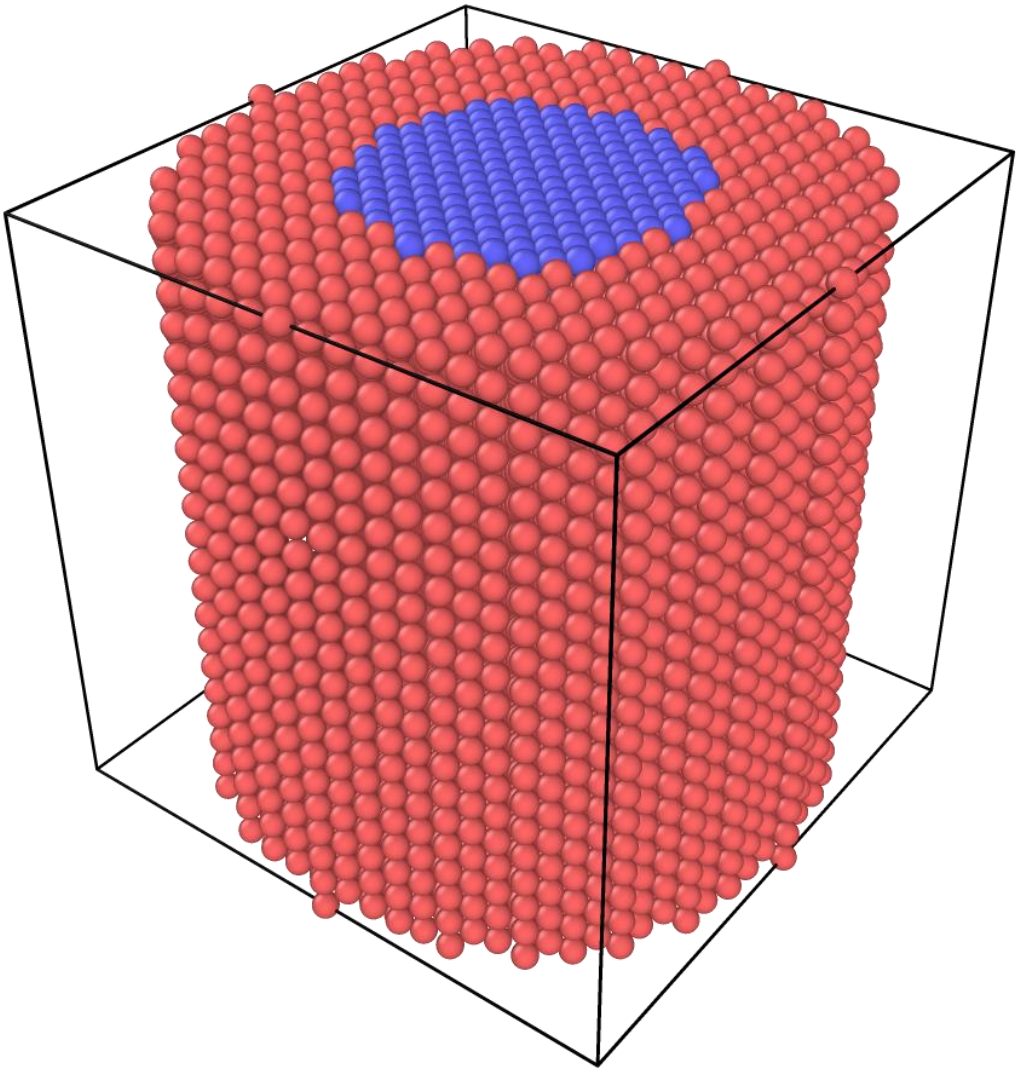

Figure 11 - A visual representation of a core-shell nanowire, the atoms are produced and placed using the Large-scale Atomic/Molecular Massively Parallel Simulator (LAMMPS). The resulting dump file visualized using the Open Visualization Tool (OVITO). All atoms are Body-Centered Cubic Iron, the red and blue coloring only indicate regions, not different materials.

Appendix B

Code used to generate the Cu and Ni cube, minimize, apply temperature, and compute thermals and energies.

Copper Cube

```
# Lammps file for a Copper Cube
# Uses Polak-Ribiere version of the conjugate gradient for minimization
# Uses Nosé-Hoover (isothermal-isobaric) to calculate Temperature

# Frank Braaksma - April 2019

# Variable Declaration
variable    side  equal 16
variable    Temp    equal   300.0
variable    runtime equal   3000
variable    simsteps equal  100
variable    dt      equal   0.01

# 1. Initialization
dimension   3
boundary    p p p
units       metal
atom_style  atomic
pair_style  eam/alloy
timestep    ${dt}

# 2. Atom definition
# 2.1 Define box
lattice     fcc       3.615   #from EAM file
region          box         block   0  ${side}  0  ${side}  0  ${side}  units
lattice
create_box  1       box

# 2.2 Define atoms
create_atoms      1     region box

# 3 Settings
# 3.1 Interatomic potentials
# pair_coeff * * Cu.lammps.eam Cu - Old EAM file
pair_coeff * * CuNi_v2.eam.alloy Cu

# 3.2 Minimization
min_style   cg
minimize    1e-5 1e-5 1000 1000
reset_timestep  0

# 3.3 Initial velocity
velocity    all create ${Temp} 2546876
```

```
# 3.4 Fixes
fix        1     all  npt  temp  ${Temp}  ${Temp}  $(100.0*v_dt)  iso  0.0  0.0
$(1000.0*v_dt)

# 3.5 Compute energies
compute 1 all pe

# 3.6 Output files
thermo 1
# Print all relevant parameters - timestep, temperature, potential energy
# thermo_style custom step temp pe epair emol etotal press vol
thermo_style custom step temp pe
dump  1     all   custom  $(v_runtime/v_simsteps)  dump.cucube.lammpstrj  id
type xs ys zs
# dump      1     all   atom 1 dump.cucube.lammpstrj

# 4 Run simulation
run   ${runtime}
```

Nickel Cube

```
# Lammps file for a Nickel Cube
# Uses Polak-Ribiere version of the conjugate gradient for minimization
# Uses Nosé-Hoover (isothermal-isobaric) to calculate Temperature

# Frank Braaksma - April 2019

# Variable Declaration
variable    side  equal 16
variable    Temp    equal   300.0
variable    runtime equal   3000
variable    simsteps equal  100
variable    dt      equal   0.01

# 1. Initialization
dimension   3
boundary    p p p
units       metal
atom_style  atomic
pair_style  eam/alloy
timestep    ${dt}

# 2. Atom definition
# 2.1 Define box
lattice     fcc       3.520 #from EAM file
region            box       block   0 ${side} 0 ${side} 0 ${side} units
lattice
create_box  1       box
```

```
# 2.2 Define atoms
create_atoms      1     region box

# 3 Settings
# 3.1 Interatomic potentials
# pair_coeff * * Ni.lammps.eam Ni - Old EAM file
pair_coeff * * CuNi_v2.eam.alloy Ni

# 3.2 Minimization
min_style   cg
minimize    1e-5 1e-5 1000 1000
reset_timestep  0

# 3.3 Initial velocity
velocity    all create ${Temp} 2546876

# 3.4 Fixes
fix        1     all  npt  temp  ${Temp}  ${Temp}  $(100.0*v_dt)  iso  0.0  0.0
$(1000.0*v_dt)

# 3.5 Compute energies
compute 1 all pe

# 3.6 Output files
thermo 1
# Print all relevant parameters - timestep, temperature, potential energy
# thermo_style custom step temp pe epair emol etotal press vol
thermo_style custom step temp pe
dump  1     all   custom  $(v_runtime/v_simsteps)  dump.nicube.lammpstrj  id
type xs ys zs
# dump      1     all   atom 1 dump.nicube.lammpstrj

# 4 Run simulation
run   ${runtime}
```

The potential energy of both cubes is extracted using LAMMPS to verify that both the temperature and potential energy are no longer fluctuating.

Generation and equilibration of Cu and Ni cubes

After 3000 timesteps, which equates to 30 picoseconds, the temperature and potential energy are equilibrated. This can be seen from respectively Figure 12 and 13 for the Cu and Ni cubes.

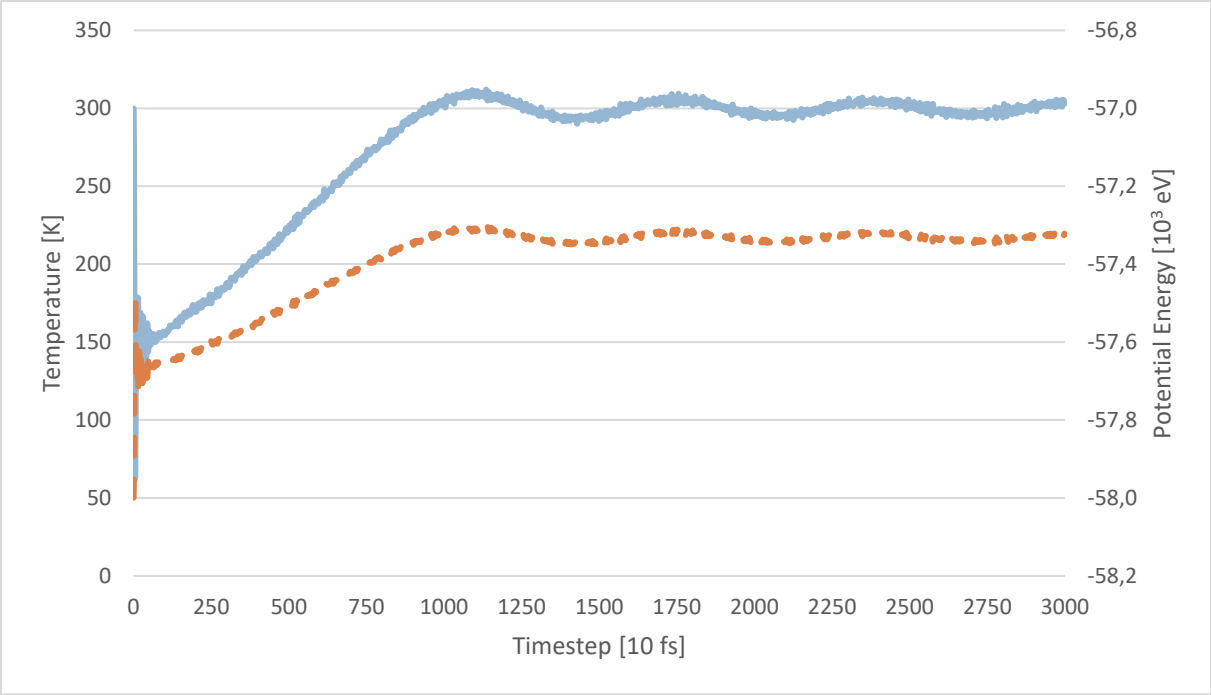

Figure 12 - Graph depicting equilibration of temperature [K] (blue, line) and Potential Energy [10³ eV] (orange, dashed) for a Cu Cube. Time [10 fs] on horizontal axis.

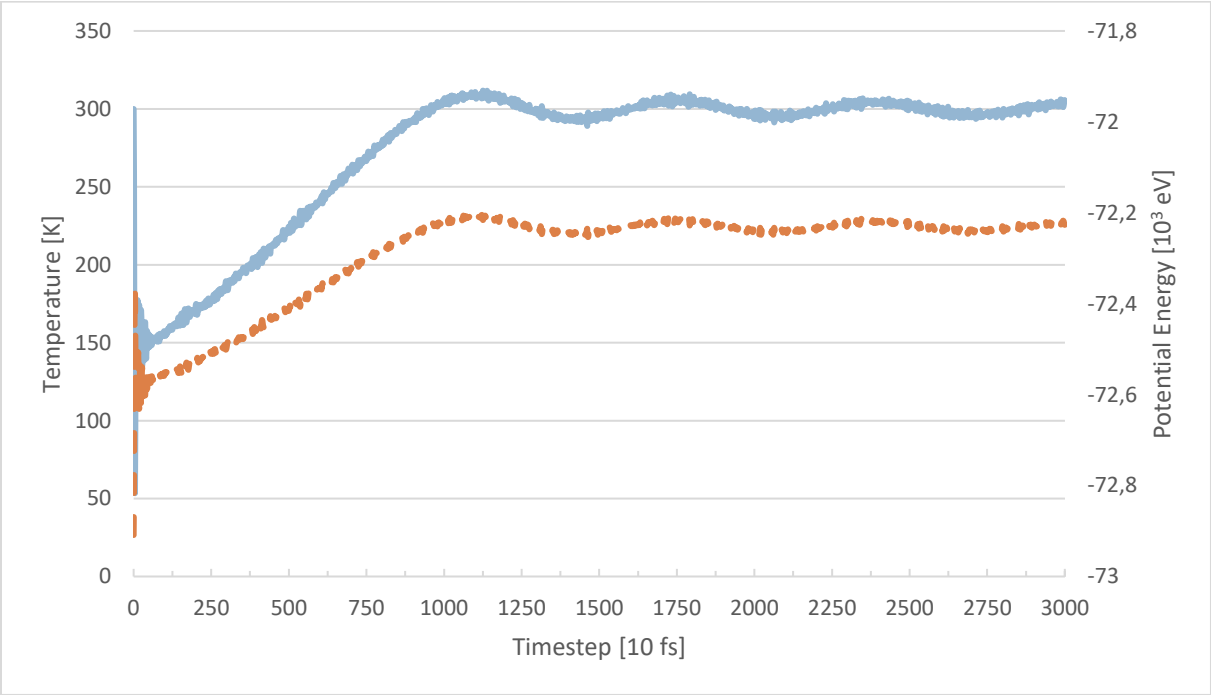

Figure 13 - Graph depicting equilibration of temperature [K] (blue, line) and Potential Energy [10³ eV] (orange, dashed) for a Ni Cube. Time [10 fs] on horizontal axis.

Radial Distribution Function (RDF)

This RDF is a curve which plots the radial density G(r) versus the radius of an atom r [Å] (Solhjoo & Vakis, 2015). A typical crystalline RDF plot consists of several peaks, which indicate the distribution of the density of atoms around a reference atom. The beginning of the first peak indicates the beginning of the first neighboring atom. The

maximum of this first peak its position; and the width its diameter [Å] (Solhjoo & Vakis, 2015).

After equilibration the atoms are spaced differently than at the beginning, the distribution of the atoms in the materials is investigated using OVITO. The Radial Distribution Function (RDF) is generated using the coordination analysis tool in OVITO to verify the spacing of the atoms. (Stukowski, 2009), see Figure 14.

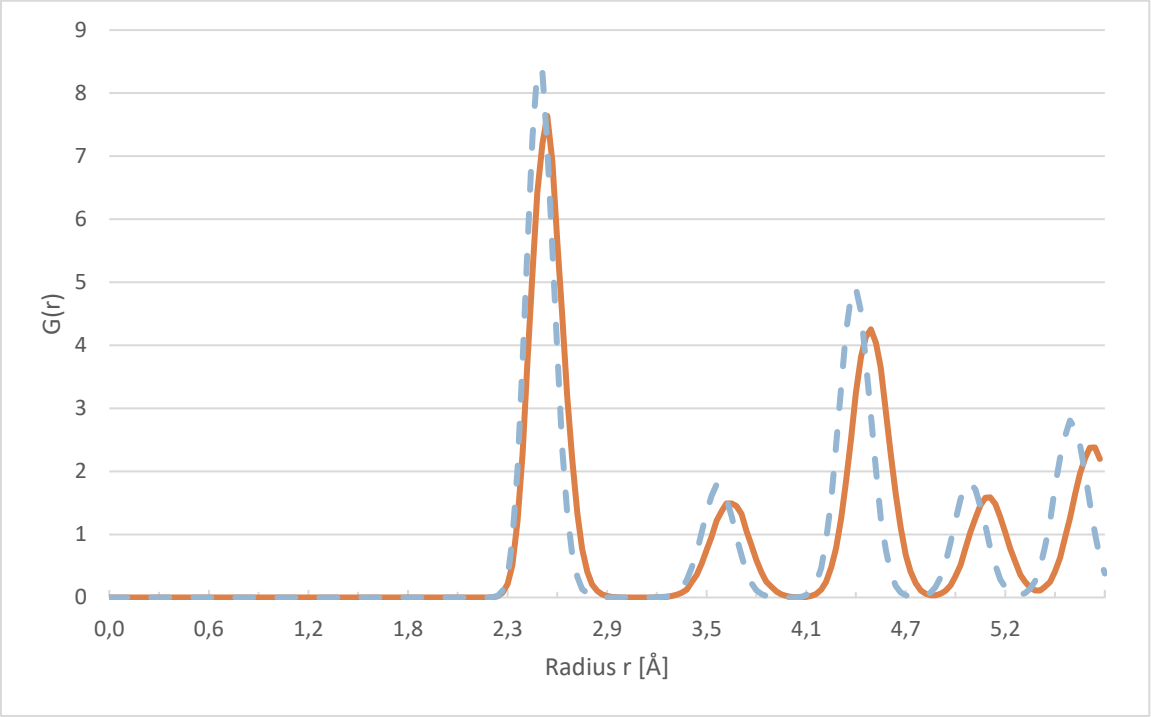

Figure 14 – RDF for Cu and Ni Cube. Distribution density G(r) of atoms plotted against radius r in Angstrom. Copper (orange, line) and Nickel (blue, dashed).

From this graph the position and width of the neighboring atoms can be found. These are presented in Table 8:

Table 8 - Values in Angstrom for the distance of atoms to a reference atom and width of atoms in the Cu and Ni cubes, extracted from the Radial Distribution Function

Material	Position [Å]	Width [Å]
Cu	2.567	0.783
Ni	2.494	0.638

Appendix C

All generated nanowires

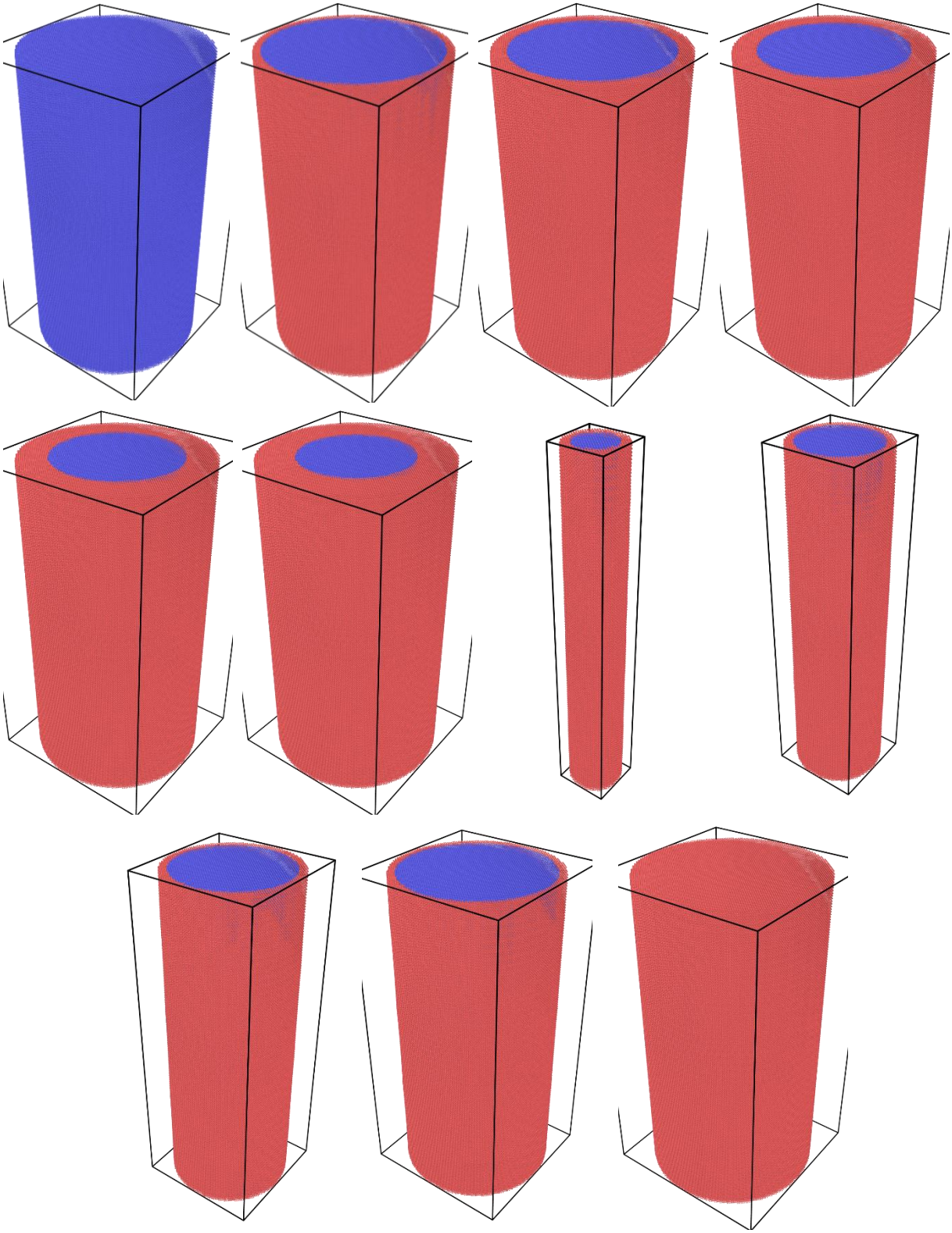

Figure 15 - All generated NWs in perspective view, generated in LAMMPS, visualized using OVITO. From top to bottom, left to right, NW 1-11

Appendix D

Figures of temperature equilibration for NWs 1-11. After generation, NWs are equilibrated for 3000 timesteps, 30 [ps], where the temperature is set to 300 [K] for the non-fixed group and 0 [K] for the fixed group.

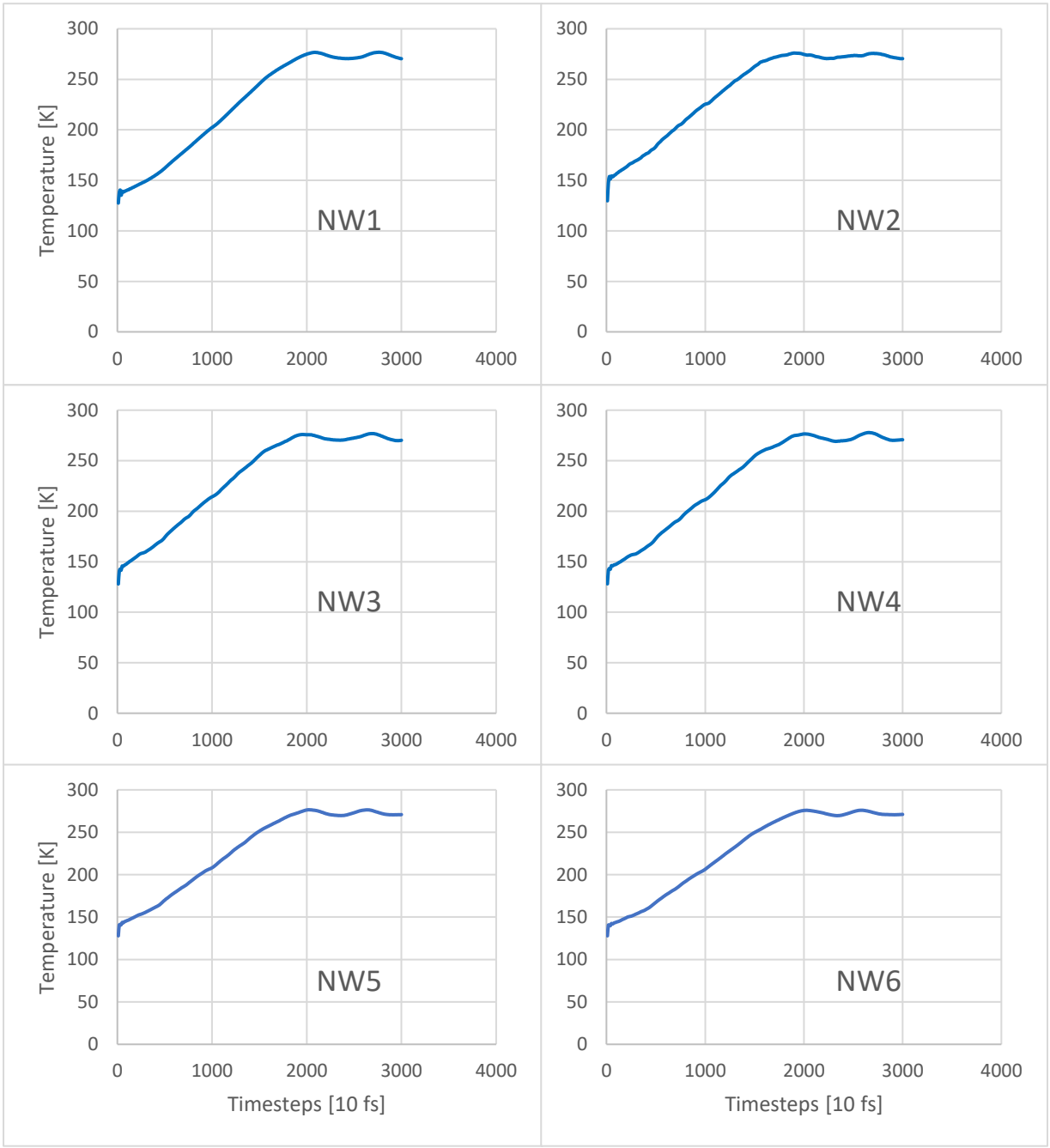

Figure 16 - Temperature equilibration graphs of NW 1-6. Temperature [K] is plotted against timesteps [10 fs]. All NWs equilibrate to ~270K.

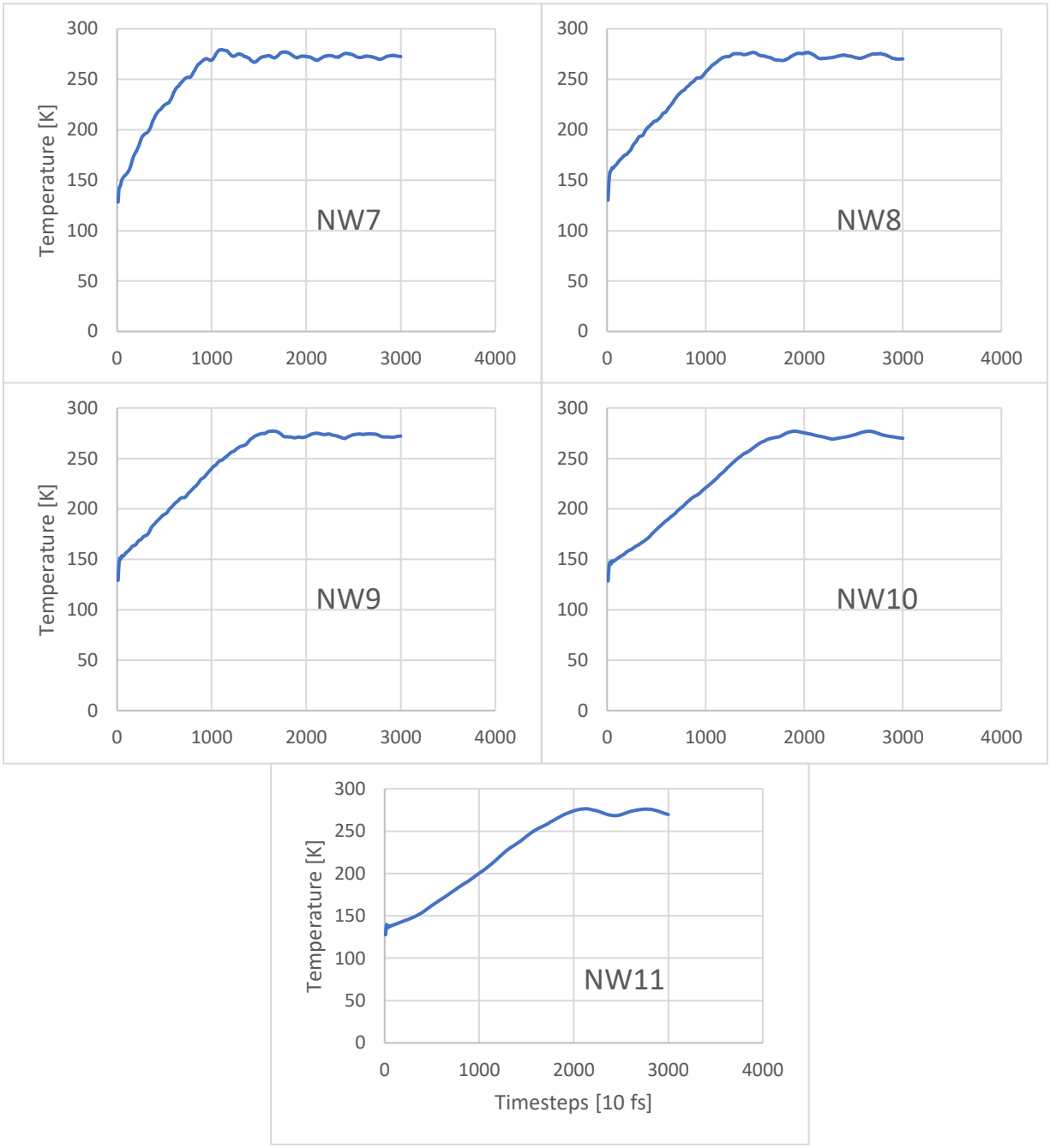

Figure 17 - Temperature equilibration graphs of NW 7-11. Temperature [K] is plotted against timesteps [10 fs]. All NWs equilibrate to ~270K.

Appendix E

Nanowire generation

Code used to generate the Cu-Ni nanowire in LAMMPS

```
# Lammps file for core-shell nanowire creation and equilibration

# Input:
# - EAM file of Copper and Nickel
# In command line the following variables:
# - Diameter of shell in [nm] (shellD)
```

```
# - Diameter of core in [nm] (coreD)
# - Number of the cylinder (cylNo)
# Output:
# - Logfile cyl(cylNo).log
# - LAMMPS trajectory file dump.cyl(cylNo).lammpstrj
# - Time-averaged values in cyl(cylNo)_EQ_timave.txt

# Frank Braaksma - June 2019

# Variable Declaration
# Material Characteristics
    variable    a0Cu    equal   3.615 #from EAM file for Copper (core)
    variable    a0Ni    equal   3.520 #from EAM file for Nickel (shell)
# Cylinder dimensions
    variable      shellDiam   equal ${shellD}*10        #Conversion of nm to
Angstrom
        variable    shellRad    equal   v_shellDiam/2   #Radius of shell
    variable      length          equal   460                 #from Sarkar &
Das paper
    variable    coreDiam    equal   ${coreD}*10         #Conversion of nm to
Angstrom
        variable    coreRad     equal   v_coreDiam/2    #Radius of core
    variable      totalDiam     equal     (${shellDiam}+${coreDiam})   #Total
Diameter
        variable    totalRad    equal   v_totalDiam/2   #Total Radius
# Fix dimensions
    variable    fixSize equal   20                      #Size in Angstrom of
fixed layer
        variable     Lo_Fx  equal     ${fixSize}           #Set bottom fixed
layer
        variable     Hi_Fx   equal    (${length}-${fixSize})  #Set top fixed
layer
# Simulation parameters
    variable     Temp         equal    300.0                #Temperature in
Kelvin
    variable    runtime     equal   3000                #Amount of timesteps
    variable     simsteps     equal    500                    #Dump every x
timesteps
    variable    dt          equal   0.01               #Length in picoseconds
of a timestep
    variable    cylCount    equal   ${cylNo}            #Number of cylinder,
from command line

# 1. Initialization
dimension   3
boundary    s s s       #shrink-wrapped in all directions
units       metal
atom_style  atomic
pair_style  eam/alloy
```

```
timestep    ${dt}

# 2. Atom definition
# 2.1 Define Box
lattice         fcc     ${a0Ni}
region          box     block 0  ${totalDiam}  0  ${totalDiam}  0  ${length}
      units box
# create_box          1     box     # Use this for 1 element
create_box      2     box     # Use this for 2 elements

# 2.2 Define atoms
# 2.2.1 Create atoms for shell
create_atoms      1       region box
region              void      cylinder z ${totalRad} ${totalRad} ${totalRad}
INF INF units box side out
delete_atoms      region      void

# 2.2.2 Create atoms for core
#-- If statement because core of 0 will exit simulation --
if "${coreRad} > 0" then &
"region             core      cylinder z ${totalRad} ${totalRad} ${coreRad}
INF INF units     box side in" &
"delete_atoms     region      core" &
"lattice         fcc        ${a0Cu}" &
"create_atoms     2       region  core" &
else "print 'MANUAL - Core is 0 or less'"

#2.3 Define Groups
region      Lo_Fx block INF INF INF INF INF ${Lo_Fx} units box
region      Hi_Fx block INF INF INF INF ${Hi_Fx} INF units box
region      Fx      union     2   Lo_Fx   Hi_Fx

group Lo_Fx region      Lo_Fx
group Hi_Fx region      Hi_Fx
group Fx        region  Fx

group   T       subtract all Fx

# 3 Settings
# 3.1 Interatomic potentials
pair_coeff * * CuNi_v2.eam.alloy Ni Cu

# 3.2 Minimization
min_style   cg
minimize    1e-5 1e-5 1000 1000
reset_timestep  0

# 3.3 Initial velocity
velocity    Fx  create  0       2345923 #Fixed region should have no velocity
```

```
velocity    T   create  ${Temp} 2344566 #Only the thermostat region should
have velocity

# 3.4 Fixes
fix     1   T nvt temp ${Temp} ${Temp} $(100.0*v_dt)

# 3.5 Output files
# 3.5.1 Print thermal data every x timesteps in log
thermo 1
# Print all relevant parameters - timestep, temperature, potential energy
thermo_style custom step temp pe
# 3.5.2 Dump all atoms in LAMMPS trajectory file
dump  1     all   custom ${simsteps} dump.cyl${cylCount}.lammpstrj id type xs
ys zs
# Alter amount of reported decimals to decrease filesize
dump_modify 1     format line "%d %d %.3f %.3f %.3f" # %.2f %.4f"

# 3.5.3 Calculate time averages and dump in text file
fix         2     T     ave/time   1   10   10   c_thermo_temp   c_thermo_pe
c_thermo_press  file  cyl${cylCount}_EQ_timave.txt  title1  "My  time-averaged
output"

# 4. Run simulation
run   ${runtime}

# Write Restart
write_restart cyl${cylCount}.EQ
```

Tensile Test

```
# Lammps file for Tensile Test of Nanowire

# Input:
# - EAM file of Copper and Nickel
# - cyl.EQ from cyl.lmp
# In command line the following variable:
# - Number of the cylinder (cylNo)
# Output:
# - Logfile TT(cylNo).log
# - LAMMPS trajectory file dump.TT(cylNo).lammpstrj
# - Time-averaged values in Temperature_Pressure_after_TT(cylNo).txt

# Frank Braaksma - June 2019

# Variable Declaration
# Simulation parameters
    variable    Temp        equal   300.0
    variable    runtime     equal   100000          #Amount of timesteps
    variable    simsteps    equal   1000            #Dump every x timesteps
    variable    dt          equal   0.01            #Duration of a timestep
in picoseconds
```

```
    variable      dfp   equal 2.566                  #From RDF
    variable      VOL   equal 4/3*PI*(v_dfp/2)^3           #dfp from RDF
    variable    cylCount    equal   ${cylNo}
    variable    str      equal   0.2             #Strain rate

# 1. Initialization
dimension   3
boundary    s s s
units       metal
atom_style  atomic

timestep    ${dt}

# 2. Atom definition
read_restart      cyl${cylCount}.EQ   #Import generated cylinder

# 2.1 Define interacting group
group    INT subtract all Fx          #Define interacting group, everything
but the Fixed group

# 3. Settings
# 3.1 Interatomic potentials
pair_style  eam/alloy                 #For some reason it would not work if
pair_style was declared at the beginning
pair_coeff * * CuNi_v2.eam.alloy Ni Cu

# 3.2 Fixes
fix      1    all nvt temp ${Temp} ${Temp} $(100.0*v_dt)   #Apply the Nose-
Hoover temperature
fix     2    Fx  setforce    0 0 0                        #Set the forces to
zero in the fixed group

# 3.3 Velocities
velocity    Hi_Fx set 0 0 +${str}  #Apply strain to top and bottom part
velocity    Lo_Fx set 0 0 -${str}

# 3.4 Computes
compute     Hi_F  Hi_Fx group/group INT  #Calculate  total  energy  and  force
between bottom Fixed part and the interacting group
compute Lo_F      Lo_Fx group/group INT  #Calculate  total  energy  and  force
between lower Fixed part and the interacting group

# 3.5 Stress Calculations
variable    tmp   equal "lz"                    #Import length of simulation
box
variable    Lz0   equal ${tmp}                  #Store in variable
variable    tmp   delete                          #Delete temporary variable
variable    strain      equal "(lz - v_Lz0)/v_Lz0"  #Calculate strain level
#-- Calculate strain in all 3 dimensions --
```

```
variable    stX   equal "-pxx/10000"
variable    stY   equal "-pyy/10000"
variable    stZ   equal "-pzz/10000"

compute           ST    all   stress/atom NULL            #Compute symmetric
per-atom stress tensor for each atom in a group
#--Calculate vonMises stress and store in variable --
variable    p1    atom  (c_ST[1]-c_ST[2])^2+(c_ST[1]-c_ST[3])^2+(c_ST[2]-
c_ST[3])^2
variable    p2    atom  6*(c_ST[4]^2+c_ST[5]^2+c_ST[6]^2)
variable    vonST   atom    sqrt((v_p1+v_p2)/2)/v_VOL/10000 #In GPa

compute           pea   all   pe/atom #Compute potential energy per atom

# 3.5 Output files
# 3.5.1 Print thermal data every x timesteps in log
thermo 10
# Print all relevant parameters - timestep, temperature, potential energy
thermo_style custom step temp pe press
# 3.5.2 Dump all atoms in LAMMPS trajectory file
fix   STPE  all   ave/atom    1   10  10  v_vonST c_pea #Add vanMises stress
calculation and Potential Energy to each atom in dump file for post-processing
dump  1     all   custom ${simsteps} dump.TT${cylCount}.lammpstrj id type xs
ys zs f_STPE[1] f_STPE[2]
dump_modify 1     format line "%d %d %.3f %.3f %.3f %.2f %.4f" #Reduce number
of decimals reported to reduce file size
# 3.5.3 Calculate time averages and dump in text file
fix         3     INT   ave/time   1   10   10   c_thermo_temp   c_thermo_pe
c_thermo_press             c_Hi_F[3]             c_Lo_F[3]             file
Temperature_Pressure_after_TT${cylCount}.txt

# 4. Run simulation
run   ${runtime}

# 4.1 Write Restart
write_restart TT${cylCount}.EQ
```

Appendix F

Strain velocity 0.4 Å/ps

Smoothed stress-strain curves, MATLAB smooth 0.005 span, for strain velocity v_{tot} = 0.4 [Å/ps].

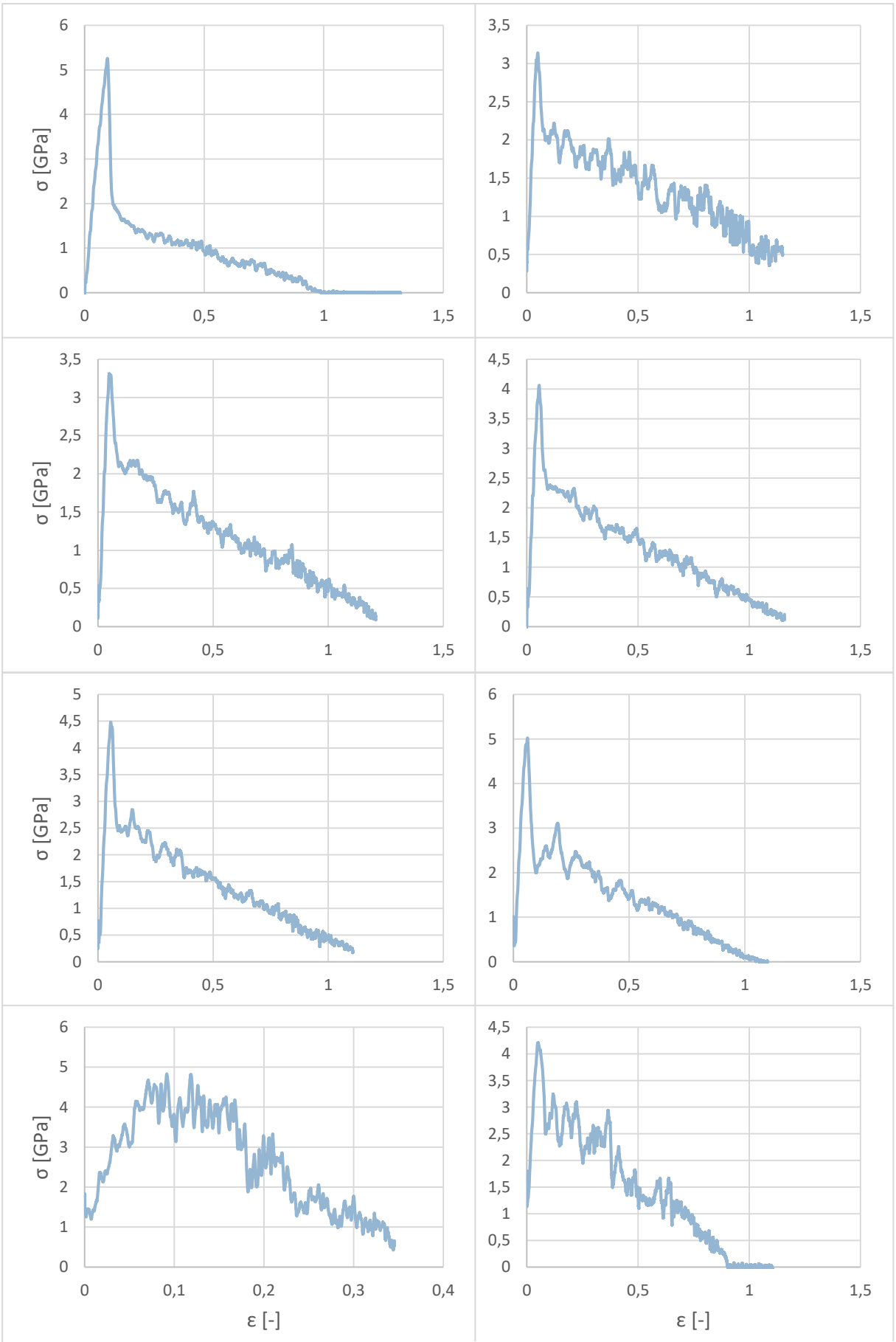

Figure 18 - Stress-strain curves for strain velocity 0.4 [Å/ps]. Top to bottom, left to right NW 1-8.

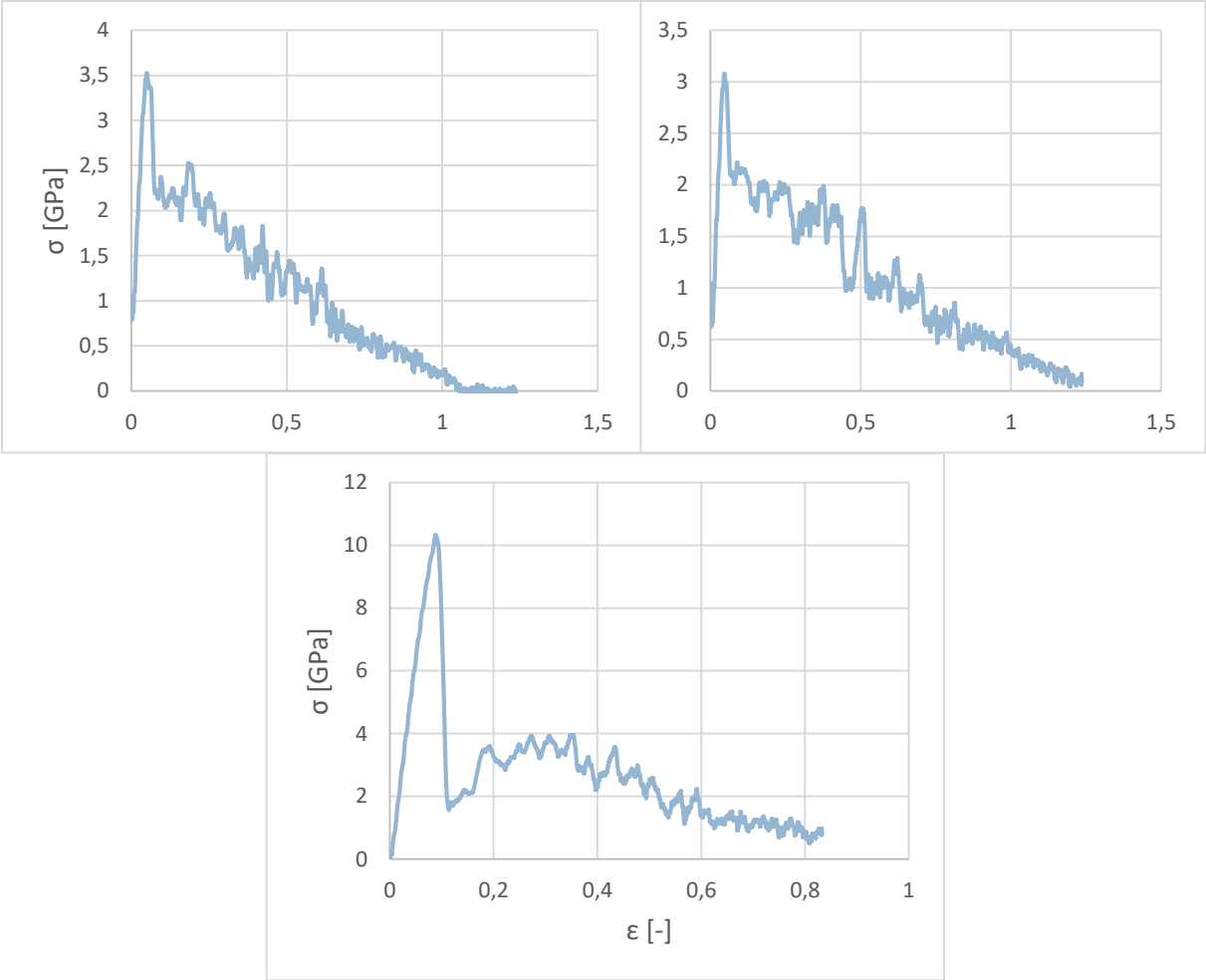

Figure 19 - Stress-strain curves for strain velocity 0.4 [Å/ps]. Top to bottom, left to right NW 9-11.

Strain velocity 1.0 Å/ps

Smoothed stress-strain curves, MATLAB smooth 0.005 span, for strain velocity v_{tot} = 1.0 [Å/ps].

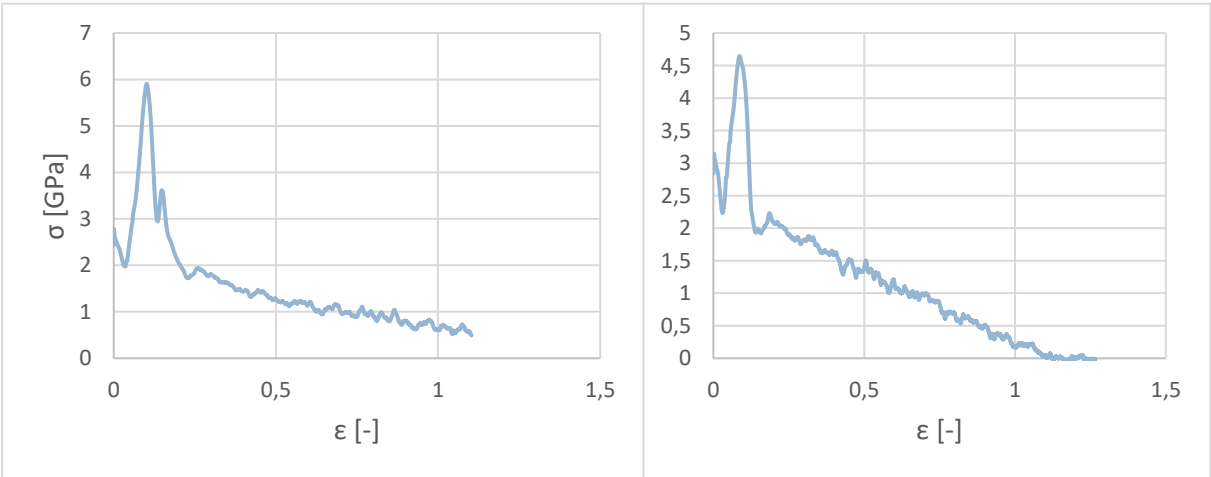

Figure 20 - Stress-strain curves for strain velocity 1.0 [Å/ps]. NW1 (left) and NW2 (right).

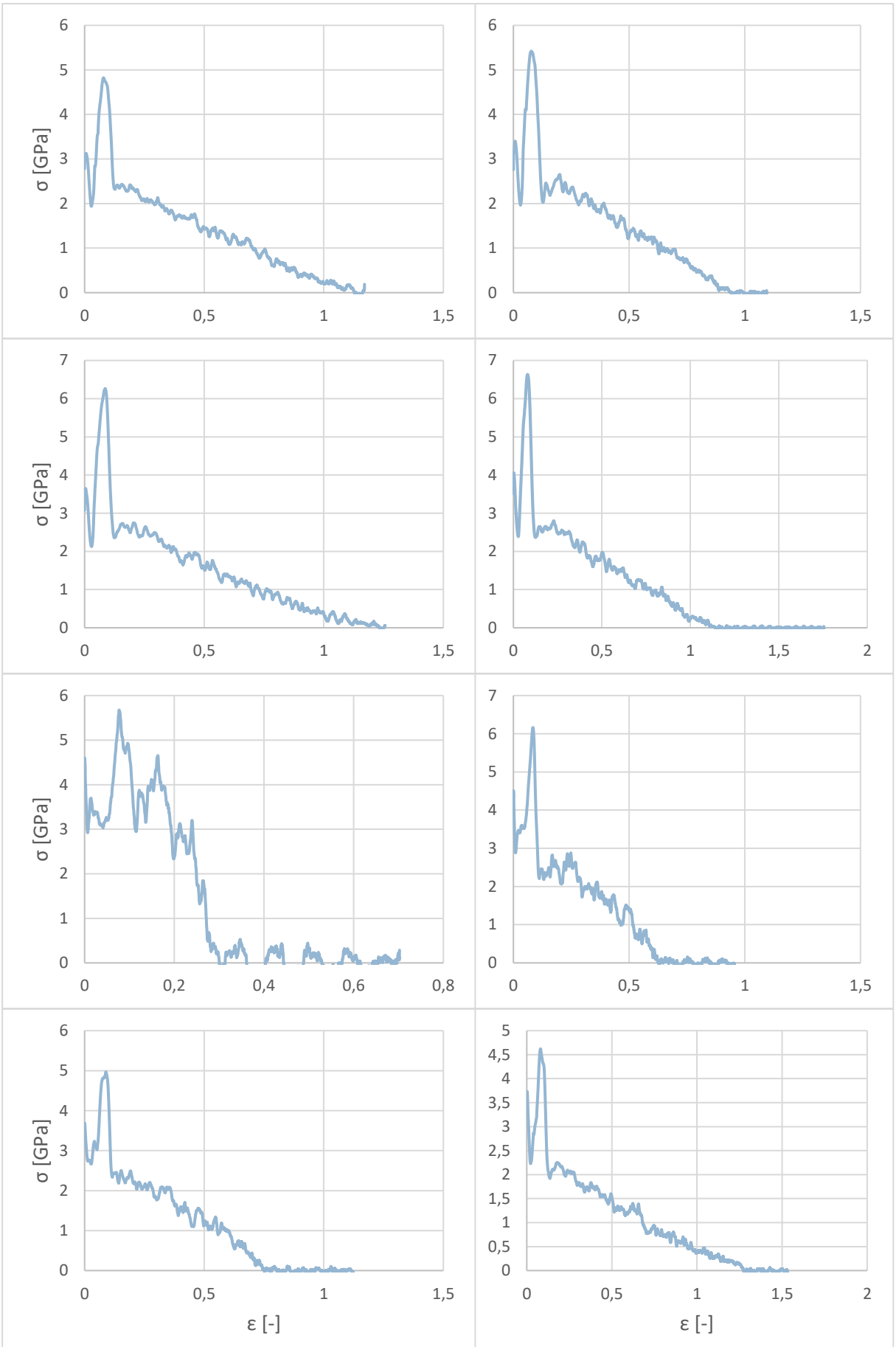

Figure 21 - Stress-strain curves for strain velocity 1.0 [Å/ps]. Top to bottom, left to right NW 3-10.

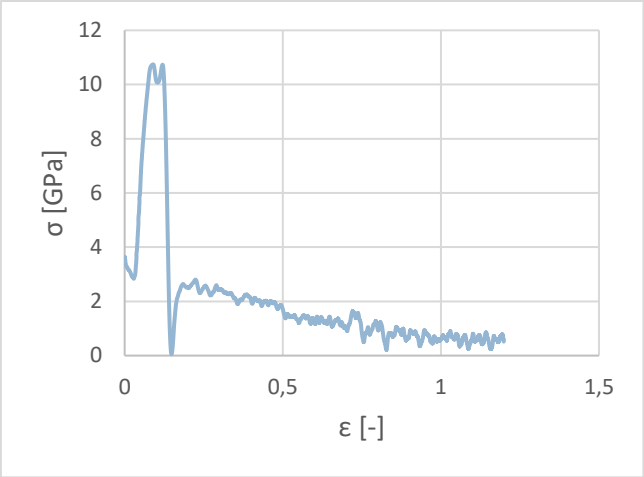

Figure 22 - Stress-strain curve for NW 11; strain velocity 1.0 [Å/ps].

Strain velocity 4.0 Å/ps

Smoothed stress-strain curves, MATLAB smooth 0.005 span, for strain velocity v_{tot} = 4.0 [Å/ps].

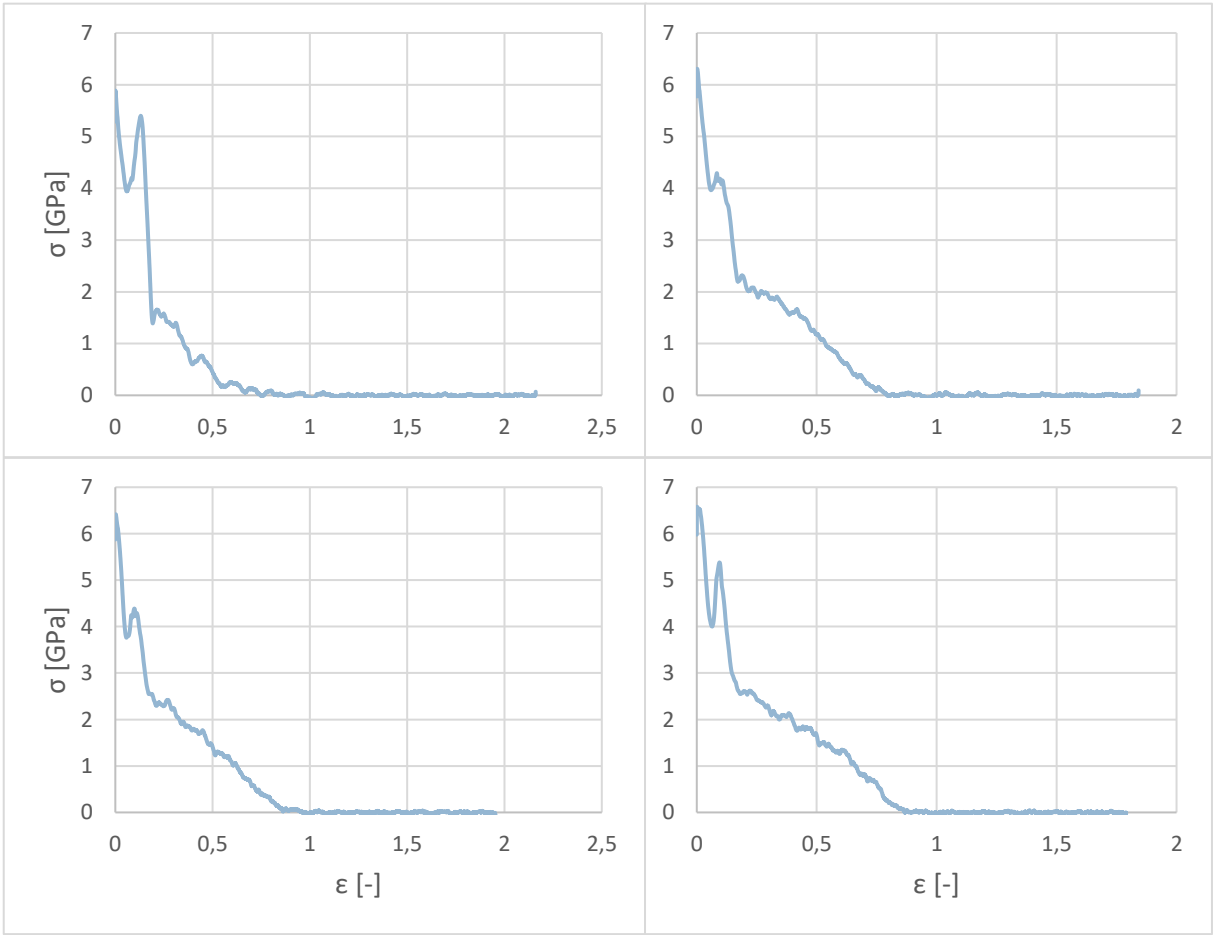

Figure 23 - Stress-strain curves for strain velocity 4.0 [Å/ps]. Top to bottom, left to right NW 1-4.

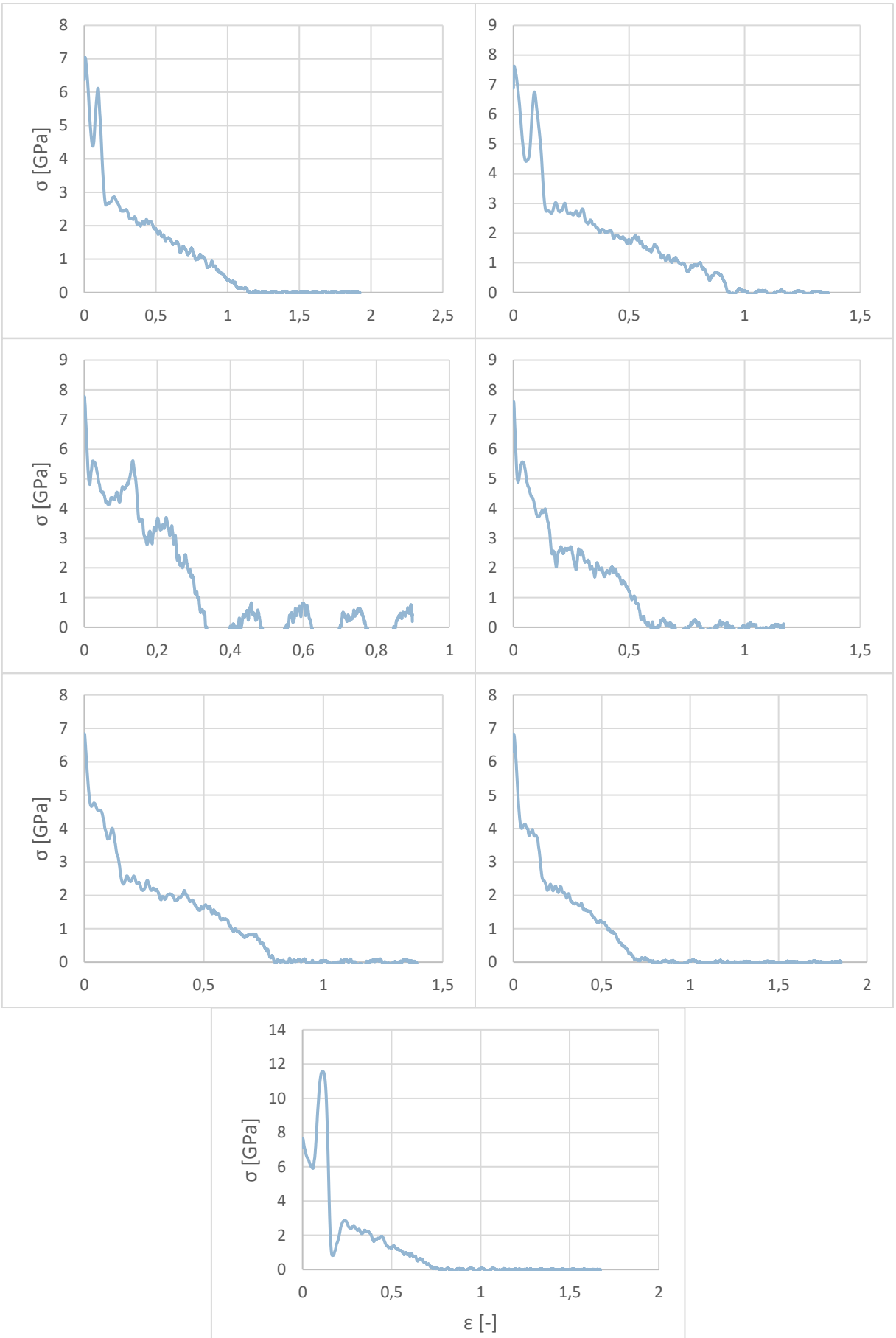

Figure 24 - Stress-strain curves for strain velocity 4.0 [Å/ps]. Top to bottom, left to right NW 5-11.